Piezo knockdown reduces 5-hydroxytryptamine release from enterochromaffin cells and exacerbates intestinal dyskinesia in mice with functional constipation

XIANGYUN YAN[1*], PEITAO MA[1*], WEN WANG[1], WEIJIAN ZENG[1], YANQIU LI[1], YUJUN HOU[1], JIANGNAN YE[1], QIANHUA ZHENG[1,2], WEI ZHANG[1], JUNPENG YAO[1,2] and YING LI[1,2]

[1]School of Acupuncture and Tuina, Chengdu University of Traditional Chinese Medicine, Chengdu, Sichuan 611137, P.R. China; [2]Key Laboratory of Acupuncture for Senile Disease, Ministry of Education, Chengdu University of Traditional Chinese Medicine, Chengdu, Sichuan 611137, P.R. China

Received April 10, 2025; Accepted August 7, 2025

DOI: 10.3892/ijmm.2025.5619

Abstract. Enterochromaffin (EC) cell dysfunction decreases 5-hydroxytryptamine (5-HT) secretion, contributing to functional constipation (FC). However, the underlying mechanisms remain unclear. Piezo ion channels mediate 5-HT release from EC cells. The present study investigated the roles and mechanisms of Piezo1 and Piezo2 in the pathogenesis of FC and explored possible interactions. In a loperamide-induced FC mouse model, Piezo1 and Piezo2 were singly or simultaneously knocked down using adeno-associated viruses. In vitro, their function in EC cells was assessed via lentiviral-mediated knockdown in the QGP-1 cell line. In FC mice, the expression of Piezo1 and Piezo2, along with their colocalization with EC cells, was significantly reduced. Knockdown of either channel impaired intestinal motility, prolonged gastrointestinal transit time, delayed gastric emptying and reduced small intestinal propulsion. Correspondingly, 5-HT, 5-HT_3 receptor and tryptophan hydroxylase-1 (TPH-1) levels were decreased. Dual knockdown exacerbated these effects, resulting in colon structural abnormalities, decreased substance P expression and increased serotonin transporter levels. Knockdown of Piezo1 or Piezo2 reduced ERK and protein kinase C (PKC) phosphorylation in colonic tissues, with combined knockdown producing a more pronounced suppression of PKC phosphorylation. Consistently, dual knockdown in EC-like cells led to more pronounced reductions in intracellular calcium, 5-HT and TPH-1 compared with single knockdowns. These findings demonstrated that Piezo1 and Piezo2 play critical and cooperative roles in maintaining intestinal homeostasis in FC mice by jointly inducing calcium ion influx in EC cells, thereby coordinating 5-HT signaling homeostasis. Targeting Piezo channels may offer novel therapeutic avenues for managing functional constipation.

Correspondence to: Professor Ying Li or Dr Junpeng Yao, School of Acupuncture and Tuina, Chengdu University of Traditional Chinese Medicine, 1166 Liutai Avenue, Wenjiang, Chengdu, Sichuan 611137, P.R. China
E-mail: liying@cdutcm.edu.cn
E-mail: yjp@cdutcm.edu.cn

Abbreviations: 5-HT, 5-hydroxytryptamine; EC, enterochromaffin cell; FC, functional constipation; AAV, adeno-associated virus; TGITT, total gastrointestinal transit time; BSFS, Bristol stool form scale score; GI, gastrointestinal; CRD, colon-rectal distension; AWR, abdominal withdrawal reflex; KD, knockdown; RNAi, RNA interference; SERT, serotonin transporter; ELISA, enzyme-linked immunosorbent assay; VIP, vasoactive intestinal peptide; SP, substance P; TPH-1, tryptophan hydroxylase-1

[*]Contributed equally

Key words: Piezo1, Piezo2, functional constipation, enterochromaffin cell, 5-hydroxytryptamine

Introduction

Functional constipation (FC) is a common, multifactorial, nonorganic disease characterized by infrequent, difficult, or incomplete bowel movements (1). FC considerably impairs the quality of life of patients and imposes a substantial burden on global healthcare systems (2,3). Epidemiological studies have estimated that the global prevalence of FC ranges from 14-20% (4,5). Despite its widespread occurrence, the underlying pathophysiological mechanisms of FC remain incompletely understood, which further complicates its effective clinical management and development of appropriate treatment strategies.

Recent advances in gastrointestinal (GI) research have identified the crucial role of enterochromaffin (EC) cells in the pathophysiology of FC (6). EC cells respond to various environmental and endogenous stimuli, including microbial metabolites, inflammatory factors, mechanical distension and stress-related hormones, by releasing serotonin [5-hydroxytryptamine (5-HT)] (7-10). Of 5-HT in the body, >90% is synthesized from tryptophan through the catalytic activity of the enzyme tryptophan hydroxylase-1 (TPH-1) in EC cells (11,12). Once synthesized, 5-HT is released into

the extracellular space, where it binds to various serotonin receptors to regulate intestinal functions, including motility, secretion and sensory perception (13-15). The activity of 5-HT is terminated predominantly through its reuptake by serotonin transporter (SERT) (16). Aberrant 5-HT release from EC cells is associated with dysregulated intestinal motility and abnormal gut sensation, which are the key contributors to the pathophysiology of FC (17,18). Notably, therapeutic agents targeting 5-HT receptors have shown substantial efficacy in alleviating constipation-related symptoms (19).

Piezo ion channels, including Piezo1 and Piezo2, are critical mechanosensors in various tissues and play a crucial role in the functional regulation of mechanosensitive cells such as EC cells (20,21). Following various mechanical stimuli, Piezo ion channels open and convert mechanical forces into cellular signals through calcium influx (22). This process regulates various cellular activities, including cell proliferation, differentiation, secretion, metabolism and signaling (23-25). Although Piezo1 and Piezo2 belong to the same Piezo family, they exhibit distinct distribution patterns in the digestive system, respond differently to mechanical signals and regulate target organs uniquely (26,27). These differences suggest that Piezo1 and Piezo2 may have complementary roles in regulating GI function.

Current research has revealed that both Piezo1 and Piezo2 individually promote the release of 5-HT from EC cells, thus highlighting their key roles in GI function (21,28). However, it remains unclear whether Piezo1 or Piezo2 independently promote the pathophysiological changes associated with FC through this mechanism. Moreover, the specific contributions of Piezo1 and Piezo2 to 5-HT release and whether they interact cooperatively or independently in EC cells remain to be elucidated. Hence, the present study aimed to investigate the distinct and combined effects of Piezo1 and Piezo2 on the regulation of 5-HT release from EC cells and their involvement in the pathophysiology of FC.

Materials and methods

Mice. Male C57BL/6 mice 6-8 weeks old and weighing 20±2 g (SPF grade) were obtained from Chengdu Dashuo Experimental Animal Co., Ltd. [cat. no. SCXK (Chuan) 2020-0030 and cat. no. SCXK (Chuan) 2024-0031]. A total of 54 mice were used in the present study. Animals were acclimatized in an environment-controlled room with a temperature of 20±2˚C, humidity of 50±5% and a 12-h light/dark cycle. Food and water were provided *ad libitum* throughout the experiment. All animal experiments were conducted in accordance with ethical guidelines and were approved by the Animal Experiment Ethics Committee of Chengdu University of Traditional Chinese Medicine (approval no. 2024012).

Adeno-associated virus construction and transduction. Technical support for the adeno-associated virus (AAV) vector construction, packaging and purification was provided by Shandong Weizhen Biosciences Co., Ltd.

AAV vectors were constructed using the pAV-U6-shRNA plasmids, designed to specifically target the Piezo1 and Piezo2 genes. The plasmids were constructed with three different short hairpin (sh)RNA sequences (Table SI) targeting Piezo1 or Piezo2, each inserted into the vector under the control of the U6 promoter. The plasmids were then amplified in bacterial cultures with appropriate antibiotic selection (Amp; 100 μg/ml) and extracted using standard plasmid purification techniques. Following plasmid extraction, the AAV vectors were packaged in 293 cells (Shandong Weizhen Biosciences Co., Ltd.) using a third-generation packaging system with a triple plasmid transfection system, according to the manufacturer's instructions. For each transfection, 10 μg of transfer plasmid, 6 μg of packaging plasmid, and 3 μg of envelope plasmid were used, at a ratio of 10:6:3. Viral particles were harvested at 72 h post-transfection. The packaged AAV particles were subsequently purified and titers were determined using reverse transcription-quantitative (RT-q) PCR.

Two weeks prior to model induction, AAV transduction was performed on colonic epithelial cells via enema, following the protocol described below. Mice were fasted for 24 h before the procedure and anesthetized using isoflurane (2% for induction and 1-1.5% for maintenance). A stainless steel round-tip needle was gently inserted approximately 2.5 cm into the colon via the anus. Subsequently, 300 μl of 20 mM N-acetylcysteine solution was slowly infused into the colon to cleanse the area, with the solution retained for 30 min. After re-anesthesia, 600 μl of AAV (total dose: $5x10^{10}$ vg per mouse) was administered into the colon via the same route. To facilitate uniform distribution of the viral vector along the colonic mucosa, several standardized procedures were employed: i) deep catheter insertion, ii) a relatively large infusion volume (600 μl), iii) temporary anal closure and iv) inversion of the mice into a vertical position for at least one min. After full recovery from anesthesia, mice were returned to their cages with free access to food and water. The time interval between AAV transduction and subsequent experimentation (model induction) was 2 weeks.

Animal model. A loperamide-induced mouse model was used to establish functional constipation, given its well-established reliability and reproducibility in gastrointestinal research. This model closely mimics the core pathophysiological features of human slow-transit constipation, including delayed colonic transit, decreased fecal water content and altered serotonergic signaling. Its technical simplicity and consistency also make it suitable for evaluating gut motility and related molecular mechanisms in experimental settings (29).

Male mice in the FC group were administered loperamide (10 mg/kg) twice daily by gavage for 14 days, while control mice received an equivalent volume of physiological saline by gavage. After one week of adaptive feeding, 54 mice were divided randomly into 6 groups: Control group, FC group, Control AAV group, AAV Piezo1-knockdown (KD) group, AAV Piezo2-KD group and AAV Piezo1/2-KD group. At the end of the modeling period, the defecation status of the mice was recorded over a 6-h period according to previously published methods (30), including the number of fecal pellets, the Bristol stool form scale score (BSFS) (31) and the fecal moisture content.

Fecal pellets were collected immediately after expulsion and placed in sealed 2-ml tubes to avoid evaporation. The fecal pellets were weighed (wet weight, in mg), dried at 60˚C overnight, and weighed again (dry weight, in mg). Fecal water

content was calculated using the equation: water content (%)=100x (wet weight-dry weight)/wet weight. Additionally, the total fecal output, BSFS and wet weight were assessed every 2 h.

At the end of the experiments, all mice were sacrificed by cervical dislocation under deep isoflurane anesthesia, in accordance with institutional ethical guidelines.

Assessment of functional GI motility. To measure total gastrointestinal transit time (TGITT), overnight-fasted mice were orally gavaged with 0.2 ml of Evans blue solution (Beijing Solarbio Science & Technology Co., Ltd.). TGITT was assessed as the time from gavage until the appearance of the first blue fecal pellet. Colonic transit time was measured by recording the time from gavage to the expulsion of the first blue fecal pellet.

To assess the small intestinal propulsive rate and gastric emptying rate, mice were sacrificed 20 min after oral gavage with the Evans blue solution. The gastric emptying rate was calculated by the total stomach weight and the net stomach weight, while the intestinal propulsion rate was calculated based on the distance the blue solution travels in the small intestine. The abdominal cavity was opened using sterile forceps and surgical scissors, and the stomach was quickly removed after ligating the gastric cardia and pylorus. The stomach was placed on filter paper, opened along the greater curvature, and rinsed with phosphate-buffered saline (PBS) at pH 7.4 (HyClone; Cytiva). Excess tissue fluids and PBS were absorbed with filter paper. The net weight of the stomachs was recorded after washing away the contents. Simultaneously, the small intestine was quickly removed and spread gently onto a piece of white paper to measure its total length and the distance traveled by the Evans blue solution. The small intestinal propulsive rate and gastric emptying rates were calculated using the following formulas:

Small intestinal propulsive rate (%)=(distance traveled by Evans blue/total length of the small intestine) x100.

Gastric emptying rate (%)=[1-(total stomach weight-net stomach weight)/total stomach weight] x100.

Colonic sensitivity assessment. Behavioral responses to Colorectal Distension (CRD) were assessed by measuring the Abdominal Withdrawal Reflex (AWR) using a semi-quantitative score in conscious animals. Mice were initially anesthetized with isoflurane and a lubricated latex balloon attached to polyethylene tubing, connected to a 1 ml syringe, was inserted into the rectum and descending colon through the anus. The tubing was secured to the tail to keep the balloon in place. After allowing the mice to recover from anesthesia for 30 min, AWR measurements were performed. Observers, blinded to the experimental conditions, visually assessed the mice's responses to graded CRD volumes (0.25, 0.35, 0.5 and 0.65 ml) and assigned AWR scores based on the following criteria: 0, no behavioral response; 1, immobility during CRD with occasional head clinching at stimulus onset; 2, mild contraction of the abdominal muscles without abdominal lifting; 3, strong contraction of the abdominal muscles and lifting of the abdomen off the platform; 4, arching of the body with lifting of the pelvic structures and scrotum.

Cell culture. QGP-1 cells were purchased from Procell Life Science & Technology Co., Ltd. (cat. no. CL-0977). The cells were divided into the following five groups: Negative control (NC), vector control (VC), LV-Piezo1 KD (Piezo1 knockdown), LV-Piezo2 KD (Piezo2 knockdown) and LV-Piezo1/2 KD (combined Piezo1 and Piezo2 knockdown) groups. Cells were cultured in OPTI-MEM medium (Gibco; Thermo Fisher Scientific, Inc.; cat. no. 51985-034) supplemented with 10% fetal bovine serum (FBS; Gibco; Thermo Fisher Scientific, Inc.; cat. no. 16000-044) and penicillin-streptomycin (Gibco; Thermo Fisher Scientific, Inc.; cat. no. P1400-100).

Lentivirus construction and cell infection. RNA interference (RNAi) construction and lentivirus particle collection were conducted according to previously described methods (32). Lentiviral vectors were packaged in 293T cells (Shanghai GeneChem Co., Ltd., China), using a third-generation packaging system. For each transfection, 20 μg of transfer plasmid, 15 μg of packaging plasmid, and 10 μg of envelope plasmid were used, at a ratio of 4:3:2. Viral particles were harvested at 72 h post-transfection. QGP-1 cells were infected with lentivirus harboring RNAi targeting Piezo1 (LV-RNAi-Piezo1), Piezo2 (LV-RNAi-Piezo2) and a control (LV-RNAi-NC) at a multiplicity of infection of 10 for 72 h. The efficiency of interference was examined by RT-qPCR and western blotting. Cells were then used for subsequent experiments 72 h post-infection (transient transduction, no antibiotic selection), including functional assays and imaging studies. The target sequences used to design the RNAi constructs are listed in Table SI.

Histological examination of colonic tissue. Distal colon tissues were fixed in 4% paraformaldehyde at 4˚C for 24 h, processed in an automatic tissue processor and embedded in paraffin. Sections of 4 μm thickness were cut using a rotary microtome. Deparaffinization was performed by immersing the sections in xylene (2x30 min), followed by rehydration in 100% ethanol (2x5 min), 95% ethanol (5 min), 85% ethanol (5 min) and 75% ethanol (5 min). The sections were rinsed for 5 min, stained with hematoxylin at 22-25˚C for 5-10 min, followed by differentiation in 1% hydrochloric acid alcohol for 3 sec and bluing in alkaline water. Eosin staining was performed at 22-25˚C for 3 min, followed by dehydration in graded ethanol, clearing in xylene and mounting with neutral resin.

Immunofluorescence staining. Immunofluorescence staining was performed to detect the co-localization and expression levels of Piezo1, Piezo2 and EC cells in distal colon. Tissues were fixed in 4% paraformaldehyde at 4˚C for 24 h, processed and embedded in paraffin. Sections of 3 μm thickness were washed with PBS (cat. no. ZLI-9062; Beijing Zhongshan Golden Bridge Biotechnology Co., Ltd.) three times at 22-25˚C for 5 min each and blocked with 3% bovine serum albumin (cat. no. GC305010; Wuhan Servicebio Technology Co., Ltd.) at 22-25˚C for 30 min. Primary antibodies used were anti-Piezo1 (cat. no. DF12083; Affinity Biosciences, Ltd.; 1:100), anti-Piezo2 (cat. no. NBP1-78624SS; Novus Biologicals; 1:200), anti-Chromogranin A (cat. no. 10529-1-AP; Proteintech Group, Inc.; 1:200) and anti-5-HT (cat. no. 20080; ImmunoStar Inc.; 1:100), the latter two of which were used to identify

EC cells. Sections were incubated with primary antibodies overnight at 4˚C, washed with PBS, and then incubated with HRP-conjugated goat anti-rabbit secondary antibodies (cat. no. GB23303; Wuhan Servicebio Technology Co., Ltd.; 1:100) or CY5-conjugated goat anti-rabbit secondary antibodies (cat. no. GB27303; Wuhan Servicebio Technology Co., Ltd.; 1:100) for 50 min at 22-25˚C. TSA reagents CY3-Tyramide (cat. no. G1223; Wuhan Servicebio Technology Co., Ltd.; 1:500) and FITC-Tyramide (cat. no. G1222; Wuhan Servicebio Technology Co., Ltd.; 1:500) were used for signal amplification for 10 min at 22-25˚C in the dark followed by PBS washes. DAPI (cat. no. G1012; Wuhan Servicebio Technology Co., Ltd.) was used for nuclear staining for 10 min at 22-25˚C in the dark followed by PBS washes. DAPI and fluorescent signals were observed under a fluorescence microscope at x200 and x400 magnifications.

Negative controls were included by omitting the primary antibodies and replacing them with equal volumes of PBS. These control sections were processed in parallel with experimental samples, including incubation with the same secondary antibodies and DAPI. No fluorescent signals were observed under these conditions, confirming the specificity of the staining.

The analyses were carried out under an Olympus VS200 digital slide scanning system (Olympus Corporation) and images were analyzed with ImageJ software (version 1.54f; National Institutes of Health) to assess the co-localization and quantify the positive expression of Piezo1, Piezo2 and EC ($ChgA^+$) cells.

Immunohistochemistry. Tissues were fixed in 4% paraformaldehyde at 4˚C for 24 h, processed and embedded in paraffin. Antigen retrieval was performed by heating sections in citrate buffer (pH 6.0, cat. no. GA2307051; Wuhan Servicebio Technology Co., Ltd.) using a microwave for 20 min. After cooling to 22-25˚C, distal colon sections were washed three times with PBS (cat. no. G0002-2L; Wuhan Servicebio Technology Co., Ltd.) for 5 min each. Endogenous peroxidase activity was quenched by incubation with 3% hydrogen peroxide (cat. no. G1204; Wuhan Servicebio Technology Co., Ltd.) at 22-25˚C in the dark for 25 min, followed by three PBS washes. Nonspecific binding was blocked with 3% bovine serum albumin (cat. no. GC305010; Wuhan Servicebio Technology Co., Ltd.) for 20 min at 22-25˚C. Sections were incubated overnight at 4˚C in a humidified chamber with the following primary antibodies: Anti-5-HT_3 (cat. no. 120185; Zen Bioscience; 1:100) and anti-SERT (cat. no. 19559-1-AP; Proteintech Group; 1:400) diluted in PBS. After PBS washes, sections were incubated with HRP-conjugated goat anti-rabbit secondary antibody (cat. no. GB23303; Wuhan Servicebio Technology Co., Ltd., 1:100) for 30 min at 37˚C. Immunoreactivity was visualized using 3,3'-diaminobenzidine (DAB) substrate (cat. no. ZLI-9018; Beijing Zhongshan Golden Bridge Biotechnology Co., Ltd.), with color development monitored under a light microscope and stopped by rinsing in distilled water. Sections were counterstained with hematoxylin (cat. no. LM10N13; J&K Scientific) for 3 min at 22-25˚C, blued in running water, dehydrated, cleared in xylene and mounted with neutral resin. IHC images for 5-HT_3 and SERT were acquired at x400 magnification using a digital trinocular microscope imaging system (cat. no. BA400Digital; Motic China Group Co., Ltd.), including both the mucosal and muscular layers of the distal colon. For each mouse, three non-overlapping fields were selected and analyzed using ImageJ software (version 1.54f; National Institutes of Health). Positive immunoreactivity was quantified as the percentage of DAB-stained area relative to the total tissue area (positive area fraction). Color deconvolution and thresholding were standardized across all images to ensure consistent measurement.

Co-immunoprecipitation (Co-IP). Colonic tissues were lysed in IP lysis buffer (cat. no. G2038; Wuhan Servicebio Technology Co., Ltd.) supplemented with PMSF (cat. no. G2008; Wuhan Servicebio Technology Co., Ltd.) and phosphatase inhibitor cocktail (cat. no. G2007; Wuhan Servicebio Technology Co., Ltd.). Lysates were centrifuged at 14,000 x g for 10 min at 4˚C and supernatants were collected. Protein concentrations were determined using a BCA Protein Assay kit (cat. no. BL521A; Biosharp Life Sciences). For each IP reaction, 400 μl of lysate was used. Protein A magnetic beads (cat. no. HY-K0203, MedChemExpress) were pre-washed three times with binding/wash buffer provided in the kit and incubated with 10 μg of anti-Piezo1 antibody (rabbit polyclonal; cat. no. 15939-1-AP; Proteintech Group, Inc.) at 4˚C for 2 h to form antibody-bead complexes. Then, 400 μl of lysate was added to the complexes and incubated for an additional 2 h at 4˚C with rotation. After four washes with binding/wash buffer, beads were collected magnetically at each wash step. Bound proteins were eluted by boiling the beads in SDS-PAGE loading buffer (cat. no. BL502B; Biosharp Life Sciences) at 95˚C for 5 min. Eluted proteins were resolved on 7% SDS-PAGE gels, transferred to PVDF membranes (cat. no. IPVH00010; MilliporeSigma) and probed with anti-Piezo2 monoclonal antibody (mouse; cat. no. HA723342; HuaAn Biotechnology) at 1:1,000. After washing, membranes were incubated with HRP-conjugated anti-mouse secondary antibody (cat. no. GB23301; Wuhan Servicebio Technology Co., Ltd.) at 1:10,000 for 1 h at 22-25˚C. Signal was detected using ECL reagents (cat. no. BL520B; Biosharp Life Sciences) and imaged using a ChemiScope 6100 system (Clinx). No epitope tag was used.

Western blotting. To measure the expression levels of Piezo1 and Piezo2 proteins in distal colon, proteins were extracted using RIPA lysis buffer (cat. no. P0013; Beyotime Institute of Biotechnology), supplemented with protease and phosphatase inhibitor cocktails, fractionated by SDS-PAGE (10% gels; 30 μg total protein per lane) and transferred onto a PVDF membrane. The membrane was blocked with 5% skimmed milk for 30 min at room temperature. Primary antibodies were applied overnight at 4˚C: anti-Piezo1 (cat. no. DF12083; Affinity Biosciences; 1:1,000), anti-Piezo2 (cat. no. NBP1-78624, Novusbio, 1:1,000) and anti-β-actin (cat. no. AC026; ABclonal Biotech Co., Ltd.; 1:50,000)/anti-GAPDH (cat. no. ab9485; Abcam; 1:2,500). The membrane was then washed three times with TBST (0.1% Tween-20) and incubated with HRP-conjugated secondary antibodies (cat. no. S0001; Affinity Biosciences; 1:5,000) for 2 h at 22-25˚C. After washing three times with TBST (0.1% Tween-20), immunoblots were developed using enhanced chemiluminescence substrate (cat. no. 17046; Chengdu

Zen-Bioscience Co., Ltd.) and imaged with a UVP imaging system (Ultra-Violet Products Ltd.). Densitometric analysis of protein bands was performed using Gel-Pro Analyzer (version 4; Media Cybernetics, Inc.).

Detection of ERK and protein kinase C (PKC) pathway proteins. Mouse colonic tissues were rinsed with ice-cold PBS to remove residual blood and then homogenized in RIPA lysis buffer (cat. no. P0013; Beyotime Institute of Biotechnology) supplemented with 1Xprotease inhibitor cocktail (cat. no. BL612A; Biosharp Life Sciences) and 1 mM phenylmethanesulfonyl fluoride (PMSF; cat. no. BL507A; Biosharp Life Sciences). Homogenization was performed using a tissue grinder (Model KZ-III-Fl; Wuhan Servicebio Technology Co., Ltd.) for 2-5 min until tissues were completely homogenized. Tissue lysates were incubated on ice for 30 min, vortexing every 10 min, followed by centrifugation at 15,805 x g for 10 min at 4˚C. Protein concentrations (30 μg per lane) were determined using a BCA protein assay kit (cat. no. BL521C; Biosharp Life Sciences). Protein samples were mixed with loading buffer (cat. no. BL502A; Biosharp Life Sciences), denatured at 95˚C for 10 min, and stored at -80˚C until use. Protein separation was performed by SDS-PAGE (10% gels) at a constant voltage of 100 V. The proteins were then transferred onto PVDF membranes (Immobilon-PSQ; MilliporeSigma) at 200 mA for 1-2 h. Membranes were blocked with 5% non-fat milk diluted in TBST buffer (0.1% Tween-20) for 2 h at 22-25˚C and then incubated overnight at 4˚C with primary antibodies: anti-ERK1/2 (cat. no. A4782; ABclonal Biotech Co., Ltd.; 1:2,000), anti-phosphorylated (p-)ERK1/2 (cat. no. 28733-1-AP; Proteintech Group, Inc.; 1:2,000), anti-PKC (cat. no. ET1608-15; HuaAn Biotechnology; 1:5,000), and anti-p-PKC (cat. no. ET1702-17; HuaAn Biotechnology; 1:2,000). After washing with TBST buffer (0.1% Tween-20) three times, membranes were incubated with HRP-conjugated secondary antibody (cat. no. AS014; ABclonal Biotech Co., Ltd.; 1:8,000) for 2 h at 22-25˚C. Protein bands were visualized using enhanced chemiluminescence substrate (cat. no. BL520B; Biosharp Life Sciences) and imaged using the Tanon 5200 Multi Chemiluminescent Imaging System (Tanon Science and Technology Co., Ltd.). Densitometric analysis of protein bands was performed using Gel-Pro Analyzer (version 4; Media Cybernetics, Inc.).

Due to antibody compatibility and differences in molecular weight, target proteins and internal controls were detected on separate membranes. However, all blots were prepared from the same set of samples and processed in parallel under identical electrophoresis, transfer and exposure conditions.

RNA isolation, cDNA synthesis and RT-qPCR. Total RNA was extracted from distal colon tissue using the Molpure Cell/Tissue Total RNA kit (Shanghai Yeasen Biotechnology Co., Ltd.). Genomic DNA was removed with a gDNA Eraser kit. cDNA was synthesized from RNA using the PrimeScript RT reagent kit (Takara Bio, Inc.). RT-qPCR was performed with TB Green Premix Ex Taq II (Takara Bio, Inc.) on a QuantStudio 3 Real-Time PCR System (Thermo Fisher Scientific, Inc.). Thermocycling conditions were as follows: an initial denaturation at 95˚C for 30 sec, followed by 45 cycles of denaturation at 95˚C for 5 sec, annealing at 55˚C for 30 sec and extension at 72˚C for 30 sec, during which fluorescence signals were acquired. All primer sequences used in the present study are listed in Table SII. Relative mRNA expression levels of Piezo1, Piezo2 and SERT were calculated using the $2^{-\Delta\Delta Cq}$ method (33), with β-actin as the internal control. Data analysis was performed using QuantStudio Design & Analysis Software (version 1.6; Thermo Fisher Scientific, Inc.). All RNA extraction, cDNA synthesis, and RT-qPCR procedures were carried out according to the manufacturers' protocols.

Calcium ion imaging. The intracellular Ca^{2+} concentration was measured using the Ca^{2+} fluorescent probe Fluo-4 AM (cat. no. S1061S; Beyotime Institute of Biotechnology). Cells were incubated with 2.5 μmol/l Fluo-4 AM diluted in HBSS solution for 40 min in an incubator. After incubation, cells were washed three times with HBSS solution. HBSS solution was added to cover the cells and they were incubated at 37˚C for 25 min. The HBSS solution was then discarded. Cells were excited at 488 nm using an inverted fluorescence microscope. Images were analyzed using ImageJ software (version 1.54f; National Institutes of Health).

Enzyme-linked immunosorbent assay (ELISA). The concentrations of 5-HT in the serum and colon, vasoactive intestinal peptide (VIP) and substance P (SP) levels in the serum were examined using ELISA kits (cat. nos. ZC-37715, ZC-38836 and ZC-37822; Shanghai Zhuocai Biotechnology Co., Ltd.) according to the manufacturer's instructions. Colonic calcium ion concentrations and tryptophan hydroxylase-1 (TPH-1) were determined using a colorimetric calcium assay kit (cat. no. C004-2-1; Nanjing Jiancheng Bioengineering Inc.; cat. no. ZC-57264; Shanghai Zhuocai Biotechnology Co., Ltd.) following the manufacturer's protocol.

Statistical analysis. Statistical analyses were conducted using GraphPad Prism version 9.0 (Dotmatics). Data normality was assessed using the Shapiro-Wilk test and Levene's test was used to verify homogeneity of variances. For group comparisons, unpaired Student's t-tests were used for two-group comparisons and one-way ANOVA followed by Tukey correction was applied for multiple group comparisons. Non-parametric tests, including the Mann-Whitney U test and Kruskal-Wallis test with Dunn's post hoc analysis, were applied to analyze data not conforming to normal distribution. Effect sizes and 95% confidence intervals were calculated where applicable. $P<0.05$ was considered to indicate a statistically significant difference.

Results

Attenuated co-localization and expression of Piezo1 and Piezo2 in enterochromaffin cells of FC mice. To investigate the expression of Piezo1 and Piezo2 within EC cells, immunofluorescence staining was performed in control and FC mouse distal colons. ChgA was primarily localized at the crypt base, exhibiting a distribution pattern similar to that of 5-HT. (Figs. 1A and S1A). In control tissues, both Piezo1 and Piezo2 were clearly expressed in the colonic epithelium and showed substantial co-localization with $ChgA^+$ cells (Fig. 1A). In FC mice, fluorescence signals for Piezo1, Piezo2 and ChgA were visibly reduced and the overlap among these markers appeared diminished. Quantification confirmed a significant decrease

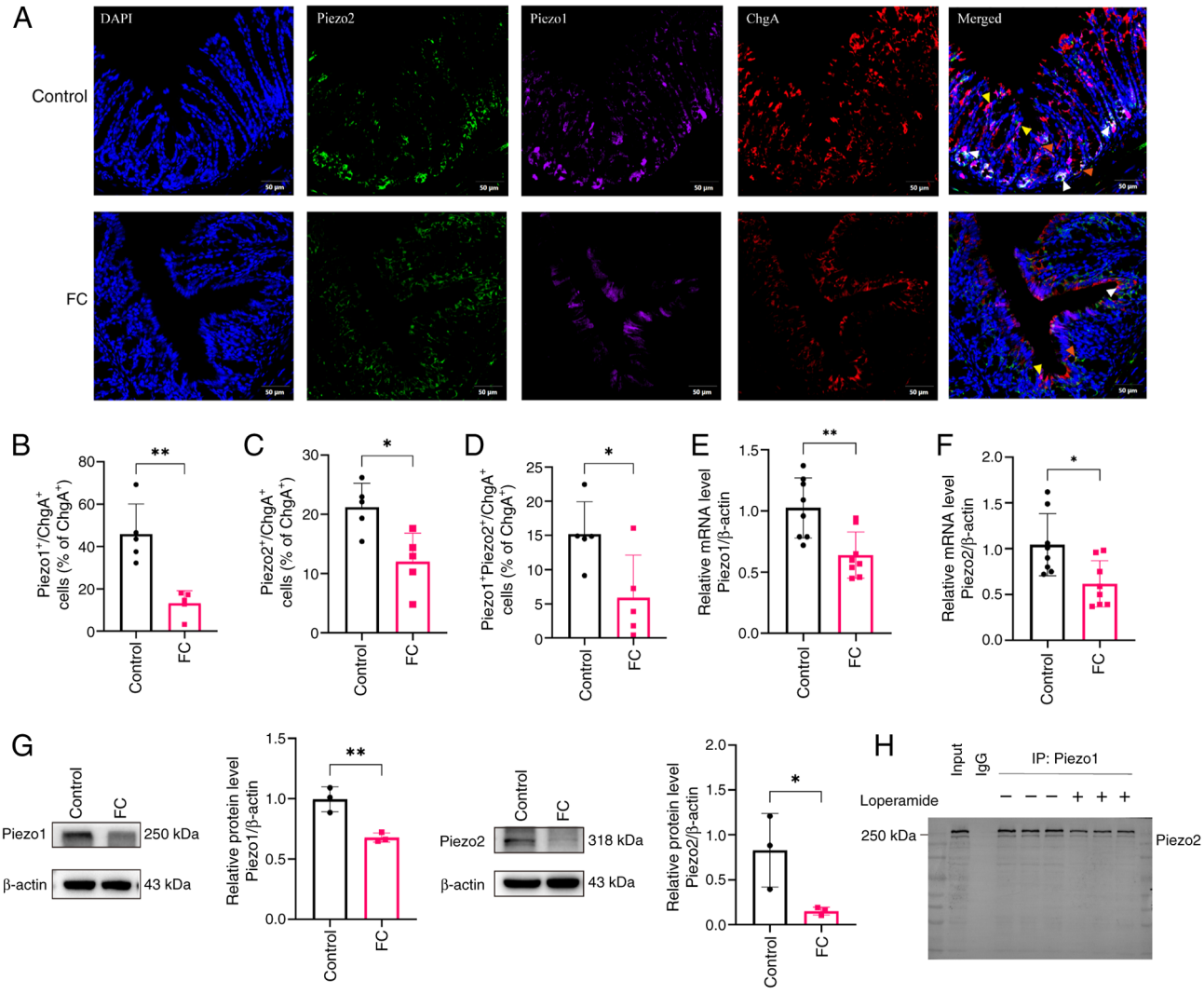

Figure 1. Colocalization and expression of Piezo1 and Piezo2 in EC cells of FC Mice. (A) Immunofluorescence staining of Piezo1, Piezo2 and EC cells in colonic sections from each group. DAPI (blue) indicates nuclei, Piezo2 (green), Piezo1 (purple) and EC cell (red). Scale bar, 50 μm (magnification, x200). Yellow arrows indicate co-localization of Piezo1 and ChgA; orange arrows indicate co-localization of Piezo2 and ChgA; white arrows indicate triple co-localization of Piezo1, Piezo2 and ChgA. Percentage of (B) Piezo1$^+$ChgA$^+$, (C) Piezo2$^+$ChgA$^+$ and (D) Piezo1$^+$Piezo2$^+$ChgA$^+$ cells as a percentage of total ChgA$^+$ cells in control and FC groups; n=5 mice per group. (E) Quantification of Piezo1 and (F) Piezo2 mRNA levels relative to β-actin in the control and FC group; n=8 mice per group. (G) Western blot analysis of Piezo1 and Piezo2 protein expression in the control and FC groups; n=3 mice per group Target proteins and internal controls were detected on separate membranes processed in parallel. The vertical line indicates membrane separation. (H) Co-immunoprecipitation of Piezo1 and Piezo2 in colonic tissues from control and FC model mice, with Piezo1 immunoprecipitated and Piezo2 detected by western blotting. Data are presented as mean ± SD and were analyzed using an unpaired two-tailed Student's t-test. Statistical significance indicated as *P<0.05, **P<0.01. EC, enterochromaffin cell; FC, functional constipation.

in the proportion of Piezo1$^+$ ChgA$^+$ cells, Piezo2$^+$ ChgA$^+$ cells and triple-positive cells among total ChgA$^+$ cells in FC mice compared with controls (Fig. 1B-D; P<0.01, P<0.05 and P<0.05, respectively), suggesting that Piezo expression in EC cells is downregulated under constipated conditions. Western blot and RT-qPCR analyses confirmed these findings, showing decreased protein and mRNA levels for both Piezo1 and Piezo2 in the FC group (Fig. 1E-G; P<0.05, P<0.01). Collectively, these results indicated that Piezos expression and Piezo1/2-EC, Piezo1-Piezo2 colocalization are significantly attenuated in FC mice.

To determine whether Piezo1 and Piezo2 physically interact under physiological and pathological conditions, Co-IP was performed using colonic tissue lysates from control and FC model mice. Piezo1 was immunoprecipitated with a specific antibody and western blotting was performed to detect Piezo2. As shown in Fig. 1H, Piezo2 was strongly detected in the immunoprecipitated fraction of control samples, confirming a specific interaction between Piezo1 and Piezo2. Notably, the intensity of the Piezo2 signal was markedly reduced in the FC group, suggesting that the pathological condition impairs the association between these two mechanosensitive ion channels. No signal was observed in the IgG control, validating the specificity of the assay.

To elucidate the roles of Piezo1 and Piezo2 in FC mice, AAV-mediated knockdown of each ion channel individually and in combination was employed (Fig. 2A). To examine the tissue distribution of AAV transduction, GFP fluorescence in colonic sections following rectal enema administration of AAV vectors was evaluated. GFP signals were mainly detectable in

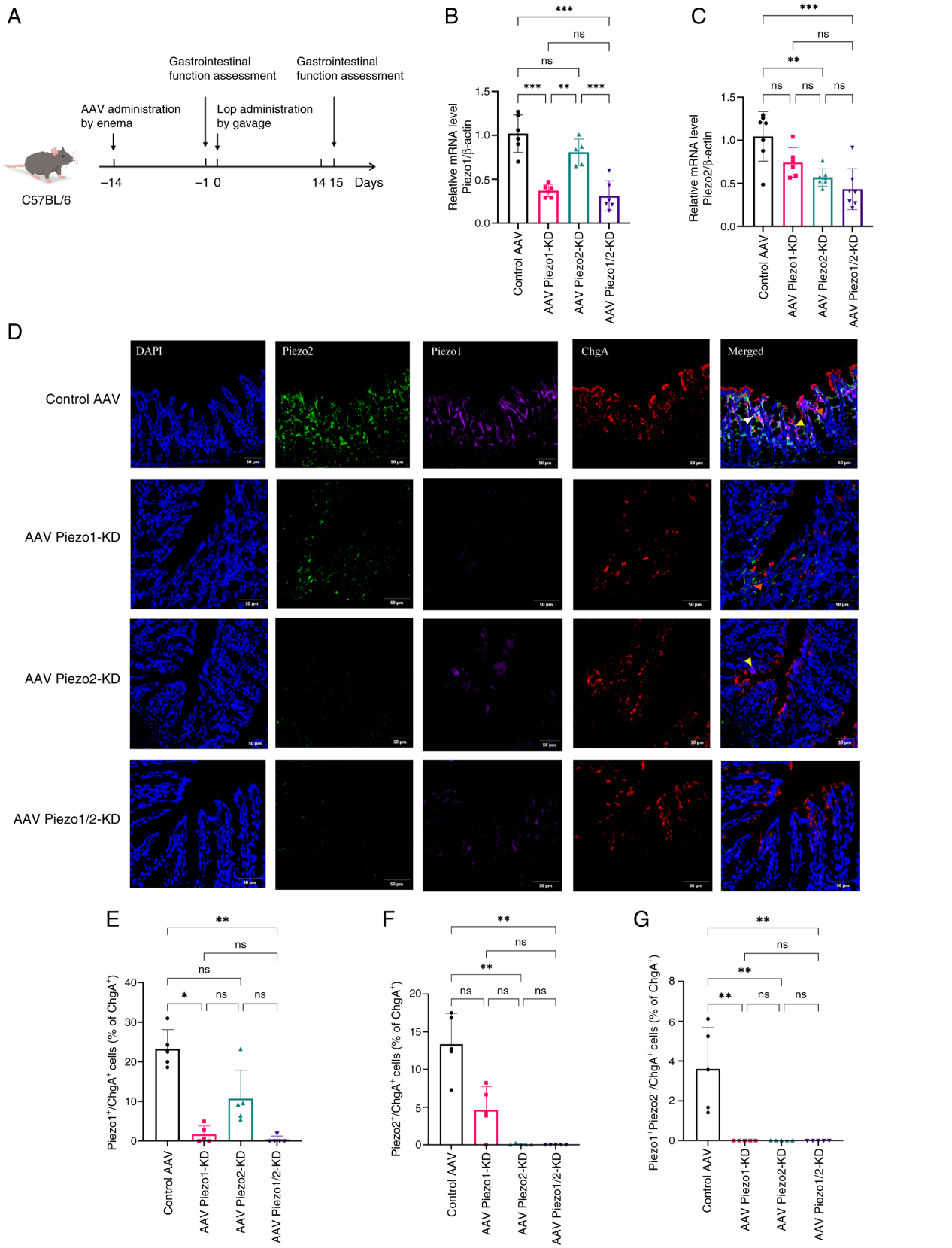

Figure 2. Piezo1/Piezo2 knockdown attenuates expression of Piezos in EC cells of FC mice. (A) Schematic of the experimental timeline for AAV-mediated knockdown. RT-qPCR analysis of (B) Piezo1 and (C) Piezo2 mRNA levels in the control AAV, AAV Piezo1-KD, AAV Piezo2-KD and AAV Piezo1/2-KD groups; n=5-7 mice per group. Data analyzed by one-way ANOVA with Tukey's post hoc test. (D) Immunofluorescence staining of Piezo1, Piezo2 and EC cells in colonic sections from each group. DAPI (blue) indicates nuclei, Piezo2 (green), Piezo1 (purple) and EC cell (red). Scale bar, 50 μm (magnification, x200). Yellow arrows indicate co-localization of Piezo1 and ChgA; orange arrows indicate co-localization of Piezo2 and ChgA; white arrows indicate triple co-localization of Piezo1, Piezo2 and ChgA. Percentage of (E) Piezo1$^+$ChgA$^+$, (F) Piezo2$^+$ChgA$^+$ and (G) Piezo1$^+$Piezo2$^+$ChgA$^+$ cells as a percentage of total ChgA$^+$ cells in control and knockdown groups; n=5 mice per group. Data represent mean ± SD and were analyzed using Kruskal-Wallis test. Statistical significance is indicated as *P<0.05, **P<0.01, ***P<0.001. ns, not significant; EC, enterochromaffin cell; FC, functional constipation; AAV, adeno-associated virus; KD, knockdown.

the mucosal layer, whereas comparatively less fluorescence was observed in the muscularis layer (Fig. S1B). In alignment with this distribution pattern, quantitative analysis of Piezo1$^+$ and Piezo2$^+$ cells showed significant decreases in the mucosa of knockdown groups compared with controls, whereas no obvious changes were observed in the muscular layer (Fig. S2). These results suggested that AAV-mediated gene modulation was predominantly associated with the mucosal region under the current delivery protocol. RT-qPCR confirmed specific and effective knockdown: Piezo1-KD significantly reduced Piezo1 mRNA (P<0.001), Piezo2-KD markedly decreased Piezo2 mRNA (P<0.01) and dual KD further diminished both mRNAs (Fig. 2B and C). Immunofluorescence-based quantification showed that the proportion of Piezo1$^+$ ChgA$^+$ cells among total ChgA$^+$ cells was significantly decreased in the Piezo1-KD and Piezo1/2-KD groups (P<0.05, P<0.01), whereas Piezo2$^+$ ChgA$^+$ cells were markedly reduced in both the Piezo2-KD and Piezo1/2-KD groups (P<0.01) (Fig. 2D-F). Furthermore, the proportion of triple-positive cells (Piezo1$^+$ Piezo2$^+$ ChgA$^+$) was markedly reduced and fell below detectable levels in all knockdown groups (P<0.01) (Fig. 2G), suggesting a near-complete loss of co-localized expression of Piezo1 and Piezo2 in EC cells upon knockdown.

These findings indicated that knockdown of Piezo1 or Piezo2 effectively reduced their respective mRNAs. Furthermore, dual knockdown markedly diminished the population of Piezo1$^+$ Piezo2$^+$ ChgA$^+$ cells to undetectable levels, indicating that Piezo1 and Piezo2 are co-expressed in a subset of EC cells.

Piezo1 and Piezo2 knockdown exacerbates impaired gastrointestinal motility and colonic sensitivity in FC mice. The FC group displayed significantly reduced total fecal output, lower BSFS scores, decreased stool water content (Fig. S3) and prolonged TGITT compared with the control group (all P<0.001), collectively indicating impaired overall gastrointestinal motility. Specifically, significant delays in small intestinal transit (P<0.01) and gastric emptying rates (P<0.001) were observed, further confirming the reduction in gut motility. Regarding colonic sensitivity, the FC group required a higher gas volume to reach an AWR score of 3 (P<0.001) and showed significantly decreased AWR scores at gas volumes of 0.35, 0.50 and 0.65 ml (all P<0.05), indicating visceral hyposensitivity (Fig. 3A-E). Histological analysis revealed normal colonic architecture in the control and FC, characterized by well-organized crypt structures with no mucosal damage or inflammatory infiltration (Figs. 3F and S4A). Serum levels of VIP and SP were assessed as indirect biomarkers of altered gut contractile function, given their well-established roles in regulating intestinal smooth muscle activity (34,35). As shown in Fig. 3G and H, VIP levels were significantly elevated and SP levels were significantly reduced in the FC group compared with the control group (P<0.01).

To investigate the functional involvement of Piezo1 and Piezo2 in gastrointestinal motility and sensitivity, Piezo1 or Piezo2 were independently knocked down in FC mice and their effects on gastrointestinal parameters assessed. Piezo1 and Piezo2 knockdown both led to significantly reduced total fecal output, delayed TGITT and increased small intestinal transit rate compared with the control AAV group (all P<0.01) (Figs. S3 and 3I, K and L). Specifically, Piezo1 knockdown decreased fecal water content, while Piezo2 knockdown reduced gastric emptying rate (both P<0.05) (Figs. S3 and 3J). In terms of colonic sensitivity, Piezo2 knockdown required a higher gas volume to achieve an AWR score of 3 compared with the control group, indicating reduced sensitivity (P<0.05). The Piezo2 knockdown group displayed significantly elevated AWR scores at each gas volume. (P<0.05), while Piezo1 knockdown showed increased AWR scores only at 0.35 ml (P<0.01) (Fig. 3M). These findings suggested that both Piezo1 and Piezo2 contribute to the regulation of gastrointestinal motility, jointly influencing total fecal output and transit times. Furthermore, Piezo1 modulates fecal water content, while Piezo2 plays a role in gastric emptying rate and colonic sensitivity.

To determine whether Piezo1 and Piezo2 exert cooperative effects on gastrointestinal function, a dual knockdown of both proteins was conducted. Simultaneous knockdown of Piezo1 and Piezo2 significantly impaired gut motility and reduced colonic sensitivity compared with the control group. Notably, dual knockdown further prolonged TGITT and increased small intestinal transit rate compared with the individual knockdown of either Piezo1 or Piezo2 (both P<0.05; Fig. 3I, K and M). Additionally, dual knockdown significantly reduced total fecal output compared with Piezo1 knockdown alone (P<0.05) and decreased fecal water content compared with Piezo2 knockdown alone (P<0.05) (Fig. S3). These findings indicated that Piezo1 and Piezo2 work in cooperation to maintain optimal gastrointestinal motility and sensitivity, jointly influencing fecal output and transit time, with Piezo1 predominantly affecting fecal water content and colonic sensitivity, while Piezo2 primarily modulates gastric emptying. This cooperation underscores the complex regulatory mechanisms involving Piezo channels in gastrointestinal homeostasis and suggests potential therapeutic targets for disorders related to impaired gut motility and sensitivity.

In the Piezo1 or Piezo2 knockdown groups, mild crypt disorganization was observed compared with the control vector group. The dual Piezo1/2 knockdown group exhibited pronounced mucosal atrophy and marked crypt architectural disarray, suggesting aggravated structural damage (Fig. 3N). Quantitative analysis further confirmed that colonic crypt depth was significantly reduced in the dual knockdown group compared with both the control vector group (P<0.001) and the single knockdown groups (P<0.01 and P<0.05, respectively) (Fig. S4B).

The Piezo1 knockdown group showed no significant changes in SP or VIP levels relative to the control vector group, indicating minimal effect of Piezo1 knockdown alone. By contrast, the Piezo2 knockdown group exhibited a significant increase in VIP levels compared with the control vector group (P<0.05), while SP levels remained unchanged. Notably, in the dual Piezo1/2 knockdown group, SP levels were significantly reduced (P<0.01) and VIP levels were further elevated (P<0.01) compared with the control vector group (Fig. 3O and P). These results indicated that changes in neuropeptide expression became more pronounced under combined Piezo1 and Piezo2 knockdown compared with single-gene knockdown.

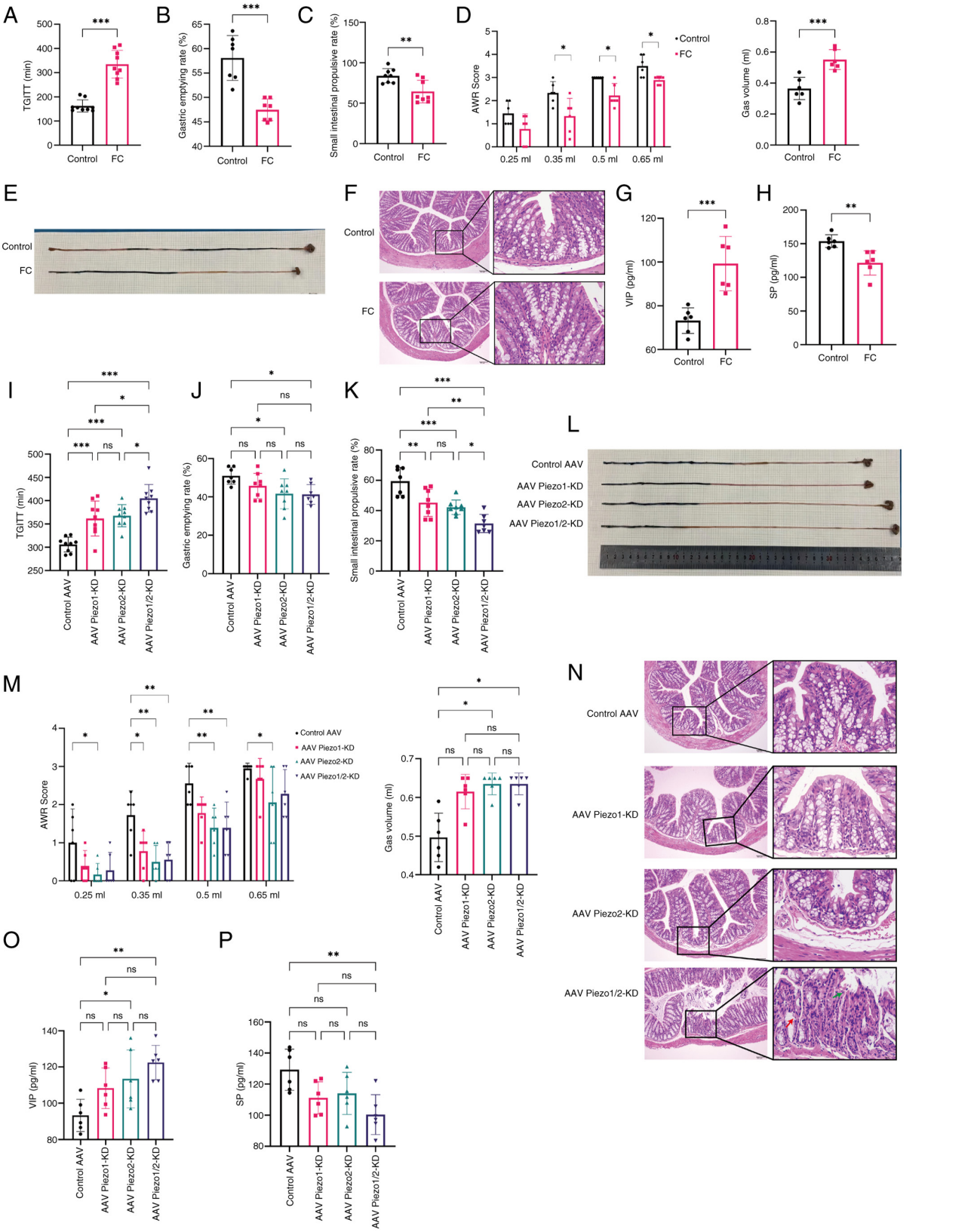

Figure 3. Effects of Piezo1 and Piezo2 knockdown on gastrointestinal motility and colonic sensitivity in FC Mice. (A-H) General effects of the FC model compared with control mice. Data were analyzed using an unpaired two-tailed Student's t-test. (I-P) Effects of individual or simultaneous Piezo1 and Piezo2 knockdown on gastrointestinal motility and sensitivity in FC mice. Data were analyzed by one-way ANOVA with Tukey's post hoc test or Kruskal-Wallis test. (A and I) TGITT, (B and J) Gastric emptying rate, (C, K, E and L) Small intestinal transit rate, (D and M) Gas volume required to reach an AWR score of 3 and AWR scores at gas volumes of 0.25, 0.35, 0.50 and 0.65 ml. (F and N) Histological analysis of colonic tissue in each group; n=3 mice per group. Red arrows highlight regions of glandular necrosis with structural disorganization and green arrows indicate nuclear pyknosis and cytoplasmic dissolution. Scale bar, 100 μm (left, magnification, x100) and 10 μm (right, magnification, x400). (G and O) Serum levels of VIP in each group, (H and P) Serum levels of SP in each group. Data were analyzed using an unpaired two-tailed Student's t-test or one-way ANOVA with Tukey's post hoc test. n=6-9 mice per group. Data represent mean ± SD. Statistical significance is indicated as *P<0.05, **P<0.01, ***P<0.001. FC, functional constipation; TGITT, total gastrointestinal transit time; AWR, abdominal withdrawal reflex VIP, vasoactive intestinal peptide; SP, substance P.

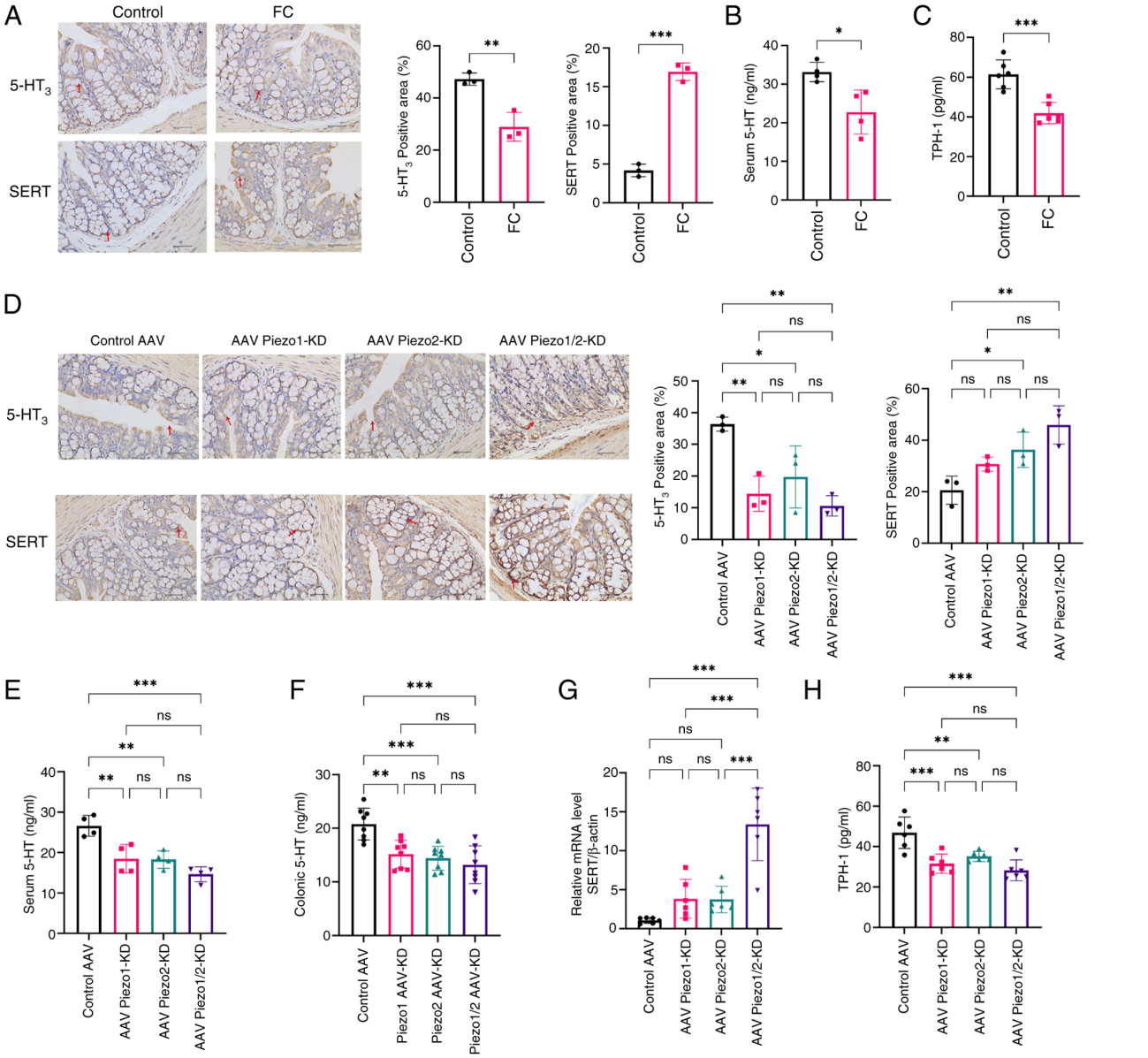

Figure 4. Effects of Piezo1 and Piezo2 knockdown on 5-HT synthesis, release and SERT expression in FC Mice. (A) Representative immunohistochemical staining of 5-HT_3 and SERT in colonic sections from control and FC mice. Scale bar, 40 μm (magnification, x400). Quantification of (B) serum 5-HT and (C) colonic TPH-1 levels in control and FC mice. Data were analyzed using an unpaired two-tailed Student's t-test; n=4-6 mice per group. (D) Immunohistochemical staining of 5-HT_3 and SERT in colonic sections from control AAV, AAV Piezo1-KD, AAV Piezo2-KD and AAV Piezo1/2-KD groups. n=3 mice per group. Scale bar, 40 μm (magnification, x400). (E and F) Serum and colonic 5-HT levels in each group, comparing knockdown groups to the control AAV group. (G and H) Relative mRNA levels of SERT and colonic TPH-1 levels in each group, comparing knockdown groups to the control AAV. Data were analyzed by one-way ANOVA with Tukey's post hoc test. n=4-6 mice per group. Data are presented as mean ± SD, with statistical significance indicated as *P<0.05, **P<0.01, ***P<0.001. 5-HT, 5-hydroxytryptamine; SERT, serotonin transporter; FC, functional constipation; TPH-1, tryptophan hydroxylase-1; AAV, adeno-associated virus; KD, knockdown.

Piezo1 and Piezo2 knockdown reduces colonic 5-HT synthesis, release and increases serotonin transporter (SERT) in FC mice. To examine the effect of Piezo1 and Piezo2 knockdown on 5-HT synthesis, release and SERT expression in the colons of FC mice, we performed immunohistochemical analysis, ELISA and RT-qPCR for related genes. Immunohistochemical staining showed a significant reduction in the percentage of 5-hydroxytryptamine receptor 3 (5-HT_3)-positive and a significant increase in the percentage of SERT-positive areas in the FC group compared with controls (P<0.01, P<0.001), indicating impaired serotonergic function in FC mice (Fig. 4A). Consistent with these findings, serum 5-HT levels were also significantly lower in the FC group compared with the control (P<0.05; Fig. 4B), while colonic TPH-1 levels, a key enzyme in 5-HT synthesis, were significantly reduced as well (P<0.001; Fig. 4C).

In the knockdown groups (Fig. 4D), 5-HT_3 and SERT expression levels varied based on the specific knockdown of Piezo1, Piezo2, or both. Quantitative analysis showed that the 5-HT_3-positive area was significantly lower in the Piezo1-KD, Piezo2-KD and combined Piezo1/2-KD groups compared with the control AAV group (all P<0.05), while no significant differences were observed between the knockdown groups. Similarly, SERT-positive area was significantly increased in Piezo2-KD and Piezo1/2-KD compared with the control AAV

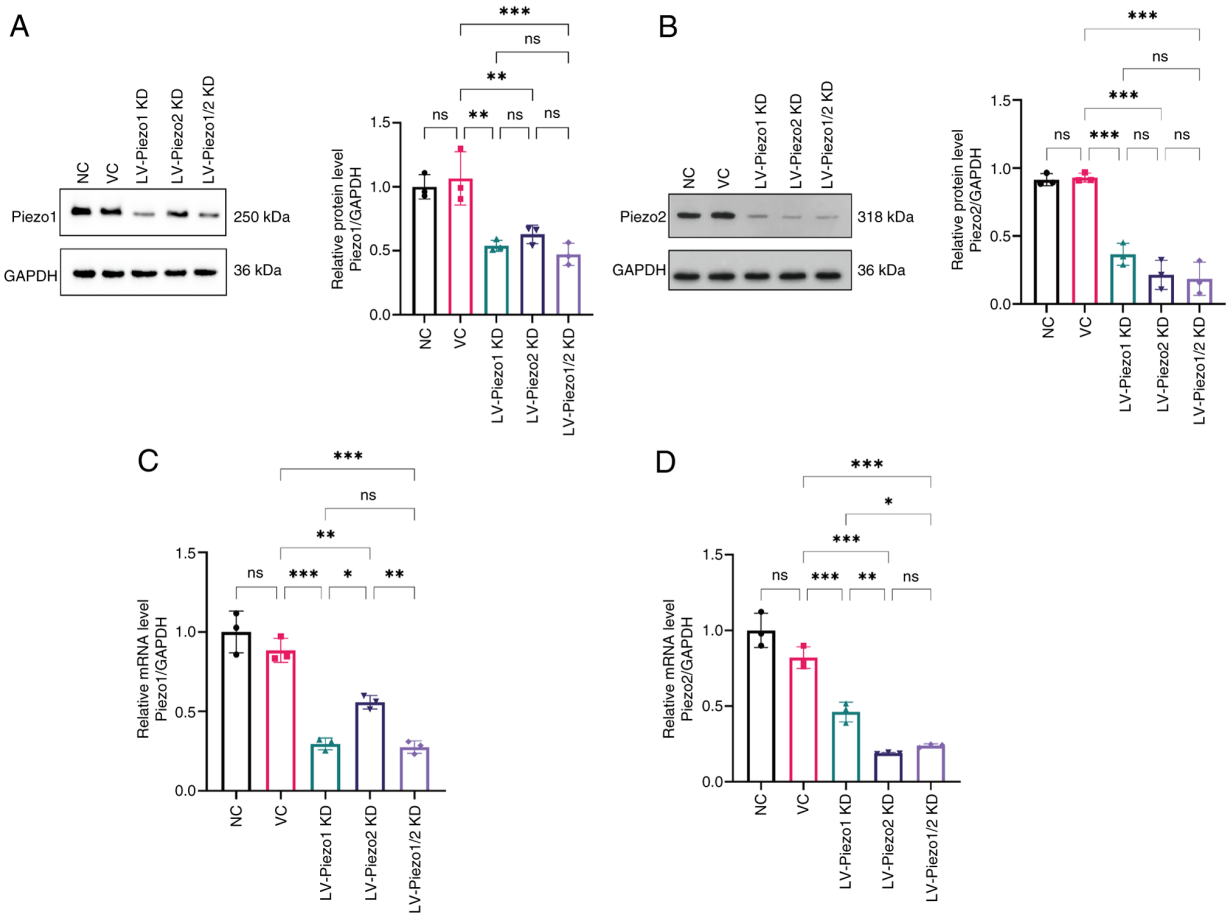

Figure 5. Expression changes of Piezo1 and Piezo2 in EC cells following individual and combined knockdown. Representative Western blot analysis of (A) Piezo1 and (B) Piezo2 protein expression in the NC, VC, LV-Piezo1 KD (Piezo1 knockdown), LV-Piezo2 KD (Piezo2 knockdown) and LV-Piezo1/2 KD (combined Piezo1 and Piezo2 knockdown) groups. GAPDH served as the loading control. Target proteins and internal controls were detected on separate membranes processed in parallel. The vertical line indicates membrane separation. Quantification of (C) Piezo1 and (D) Piezo2 mRNA levels relative to GAPDH; n=3 cells per group. Data are presented as mean ± SD and were analyzed by one-way ANOVA with Tukey's post hoc test. Statistical significance indicated as *P<0.05, **P<0.01, ***P<0.001. EC, enterochromaffin cell; NC, negative control; VC, vector control; KD, knockdown.

group (both P<0.05), with no significant differences between the individual knockdown and combined knockdown groups.

As serum 5-HT levels reflect both free and platelet-stored serotonin and may not accurately represent local biosynthesis or signaling activity, serotonergic activity in colonic tissues was further evaluated by measuring tissue 5-HT levels using ELISA. As shown in Fig. 4E and F, both serum and colonic 5-HT levels were significantly reduced in all knockdown groups compared with the control AAV group (P<0.01), with no significant differences between the knockdown groups. The mRNA levels of SERT were significantly increased only in combined Piezo1/2-KD group, compared with both the control AAV group and the individual knockdown groups (Fig. 4G, P<0.001). Furthermore, TPH-1 was reduced in all knockdown groups (Fig. 4H, P<0.01), suggesting that Piezo1 and Piezo2 are involved in maintaining 5-HT synthesis and secretion in the colonic tissue of FC mice.

Additionally, calcium levels and ERK/PKC phosphorylation in colonic tissue were assessed to explore the downstream signaling events that may be involved in Piezo-regulated 5-HT synthesis (Fig. S5). Colonic Ca^{2+} levels were significantly reduced in FC mice and further decreased in the Piezo1 and Piezo1/2 knockdown groups, with the lowest levels observed in the double knockdown group. Western blotting showed that p-ERK/total ERK and p-PKC/total PKC ratios were decreased in FC mice (Fig. S5C and D, P<0.001) and further suppressed in Piezo knockdown groups (Fig. S5E and F, P<0.001, P<0.01, P<0.05). Notably, the reduction in p-PKC/total PKC was more pronounced in the Piezo1/2-KD group compared with either single knockdown group (P<0.05). By contrast, total ERK1/2 and PKC remained unchanged.

These results collectively indicated that knockdown of Piezo1 and Piezo2 disrupted the synthesis and release of 5-HT in the colon, potentially via ERK/PKC signaling pathways associated with altered calcium levels.

Piezo1/2 expression of Piezo1 and Piezo2 knockdown in EC-like cells. To more directly investigate how Piezo channels affect 5-HT release from EC cells, *in vitro* experiments were conducted. Lentivirus-mediated knockdown targeting each protein was used (Fig. 5A-D). In the LV-Piezo1 KD group, Piezo1 protein and mRNA levels were significantly reduced compared with the control (P<0.01 and P<0.001), confirming successful knockdown. Similarly, Piezo2 protein and mRNA levels were significantly reduced in the LV-Piezo2 KD group (P<0.001).

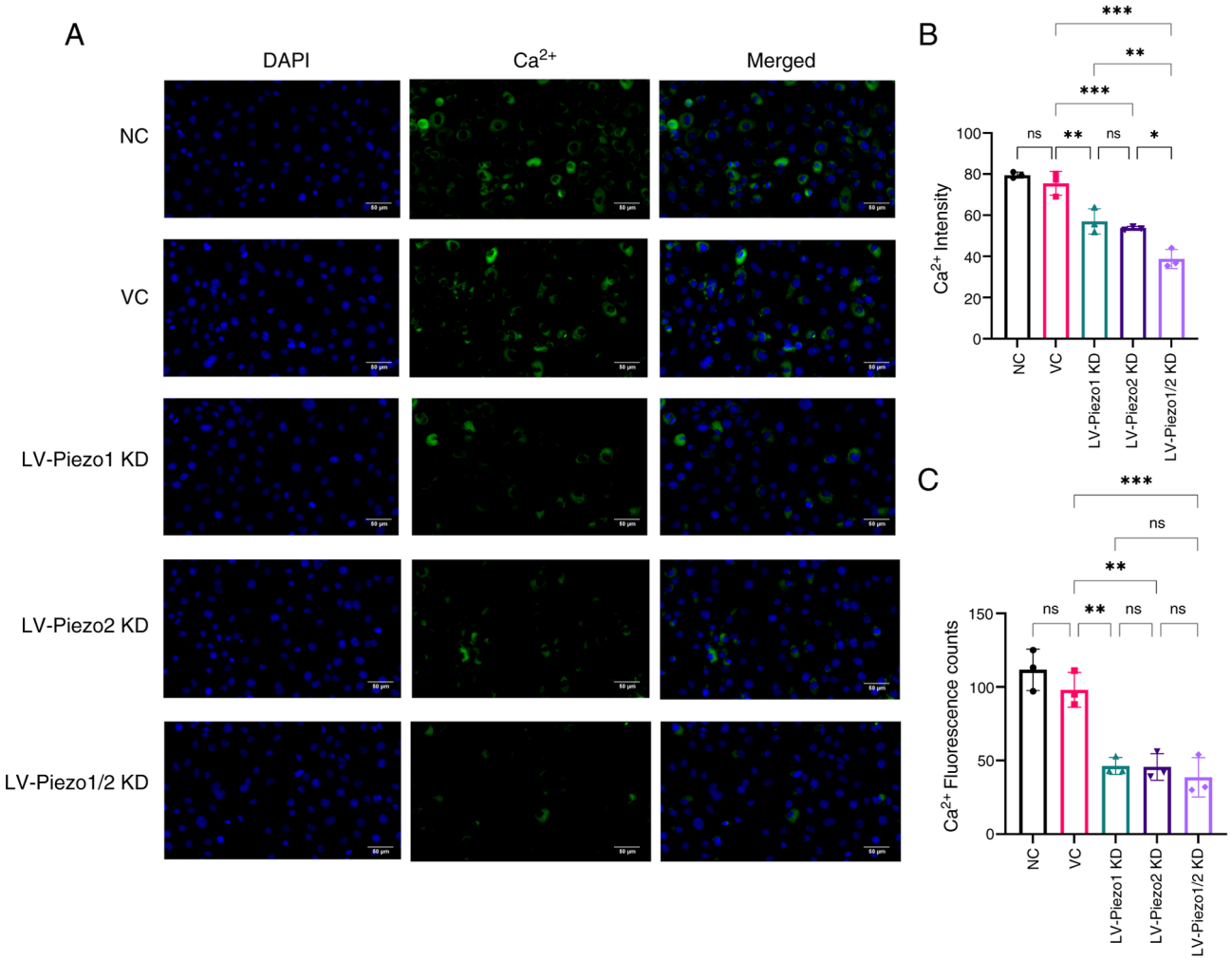

Figure 6. Effect of Piezo1 and Piezo2 knockdown on intracellular Ca^{2+} levels in ECs. (A) Representative immunofluorescence images of intracellular Ca^{2+} levels in different groups. DAPI (blue) was used to stain nuclei and Ca^{2+} indicator (green) shows intracellular calcium levels. Merged images display co-localization of nuclei and Ca^{2+} fluorescence. Scale bar, 50 μm (magnification, x400). (B) Quantification of Ca^{2+} fluorescence intensity in each group. (C) Quantification of Ca^{2+} fluorescence counts in each group; n=3 cells per group. Data are presented as mean ± SD and were analyzed by one-way ANOVA with Tukey's post hoc test. Statistical significance indicated as *P<0.05, **P<0.01, ***P<0.001. ns, not significant; EC, enterochromaffin cell.

Notably, Piezo2 expression was also significantly reduced in the LV-Piezo1 KD group and Piezo1 expression was reduced in the LV-Piezo2 KD group (P<0.001 and P<0.01), suggesting a regulatory relationship where knockdown of one Piezo protein affects the expression of the other. In the combined LV-Piezo1/2 KD group, Piezo1 and Piezo2 levels were comparable to those in their respective single knockdown groups, indicating that simultaneous knockdown is as effective as individual knockdowns in reducing each protein's expression.

These findings confirmed the efficacy of lentivirus-mediated knockdown for both Piezo1 and Piezo2 and suggest a potential interaction between Piezo1 and Piezo2 expression in EC-like cells.

Calcium imaging of Piezo1 and Piezo2 knockdown in EC-like cells. Calcium ions play a crucial role in various cellular processes and Piezo channels are known to be mechanosensitive ion channels that regulate calcium influx in response to mechanical stimuli in cells. To evaluate the effect of Piezo protein knockdown on channel activity, intracellular calcium concentration in EC cells was measured via immunofluorescence staining (Fig. 6A-C). The results demonstrated no significant decrease in total fluorescence intensity in the VC group compared with the NC group.

In EC-like cells with Piezo1 knockdown, a significant decrease in average fluorescence intensity and cell counts (P<0.01) was observed compared with the VC group. Similarly, Piezo2 knockdown resulted in a marked reduction in these parameters (P<0.01). These results suggested that knockdown of either Piezo1 or Piezo2 significantly reduces intracellular calcium concentration.

Notably, the simultaneous knockdown of both Piezo1 and Piezo2 led to an even more pronounced decrease in average fluorescence intensity compared with either Piezo1 or Piezo2 single knockdown groups (P<0.05). This indicated a cooperative effect, where the combined reduction of Piezo1 and Piezo2 resulted in a significantly greater decrease in intracellular calcium levels than the reduction observed with individual gene knockdowns.

Piezo1 and Piezo2 knockdown downregulates 5-HT and TPH-1 expression in EC-like cells. To further elucidate the effect of Piezo1 and Piezo2 on 5-HT synthesis and release

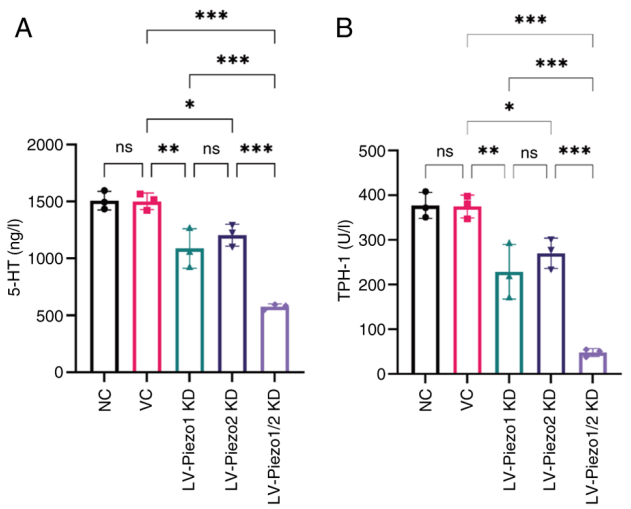

Figure 7. Effect of Piezo1 and Piezo2 knockdown on 5-HT and TPH-1 levels in enterochromaffin cells. (A) Quantification of 5-HT levels (ng/l) in the different groups. (B) Quantification of TPH-1 enzyme activity (U/l) in each group. n=3 cells per group. Data are presented as mean ± SD and were analyzed by one-way ANOVA with Tukey's post hoc test. Statistical significance indicated as *P<0.05, **P<0.01, ***P<0.001. ns, not significant; 5-HT, 5-hydroxytryptamine; NC, negative control; VC, vector control; KD, knockdown; TPH-1, tryptophan hydroxylase-1.

from EC-like cells, lentiviral-mediated knockdown of Piezo1 and Piezo2 in these cells were employed. The findings showed no significant difference in 5-HT levels between the VC group and NC group. However, knockdown of either Piezo1 or Piezo2 alone resulted in a marked decrease in both 5-HT and TPH-1 expression relative to the VC group (P<0.05). Notably, there was no significant difference in both 5-HT and TPH-1 levels between the Piezo1 and Piezo2 knockdown groups, suggesting that both proteins play similar roles in regulating 5-HT synthesis and release. Dual knockdown of Piezo1 and Piezo2 led to a further reduction in 5-HT and TPH-1 expression compared with individual knockdowns (P<0.001; Fig. 7A and B). These results suggested that Piezo1 and Piezo2 have a cooperative effect on the regulation of 5-HT and TPH-1 expression.

Discussion

Piezo channels are large trimeric mechanosensitive ion channels that transduce physical forces such as luminal distension, shear stress and peristaltic pressure into intracellular calcium signals, thereby regulating key gastrointestinal functions (36-38). They are known to influence serotonin secretion, gut motility and epithelial dynamics and have been implicated in both physiological and pathological processes including intestinal inflammation and barrier dysfunction (39-41). The present study provided both *in vivo* and *in vitro* evidence suggesting that Piezo1 and Piezo2 may act in a coordinated manner in EC cells. Their knockdown was associated with reduced intracellular calcium levels and diminished 5-HT production, along with impaired intestinal transit and reduced visceral sensitivity. These findings suggested that Piezo1 and Piezo2 contributed to gut homeostasis through EC-mediated serotonergic signaling and that their dysregulation may be involved in the pathogenesis of FC. Accordingly, targeting Piezo channels may offer a promising therapeutic strategy for restoring serotonin balance and improving GI motility in FC.

Piezo1 and Piezo2 are distributed across various cell types in the gastrointestinal tract, reflecting their involvement in multiple aspects of gut physiology. Piezo1 has been reported in epithelial cells, endothelial cells, goblet cells and smooth muscle cells (21,42,43). In the enteric nervous system, it is also expressed in cholinergic neurons along the small intestine, cecum and colon, suggesting a role in efferent neuromuscular regulation. Piezo2, by contrast, has a more selective distribution; primarily found in intrinsic primary afferent neurons and enteroendocrine cells such as ECs (44), supporting its function in mechanosensory signal input. These distinct patterns suggest that Piezo1 and Piezo2 may coordinate to regulate gut motility and sensitivity through both epithelial and neural pathways. In addition to their individual roles, Piezo channels may functionally interact with other mechanosensitive channels. Piezo1 activation facilitates TRPV4 opening via PLA2 signaling, suggesting a synergistic effect in amplifying mechanical responses (26,45), whereas TRPV1 activation inhibits Piezo activity by depleting membrane phosphoinositides, indicating an antagonistic interaction (46). Moreover, Piezo2 and TRPV1 also co-localize in colonic sensory neurons and contribute to mechanical hypersensitivity (47), implying broader crosstalk beyond epithelial pathways. The present study focused specifically on the expression and function of Piezo1 and Piezo2 in EC cells under both physiological and pathological conditions. While previous scRNA-seq studies have not reported Piezo1 expression in ECs (48), the findings of the present study supported its presence in the colonic epithelium. It was observed that Piezo1 protein co-localized with EC markers by immunofluorescence and Piezo1 mRNA expression in colonic tissue confirmed by RT-qPCR. These discrepancies may be attributed to methodological differences, as Piezo1 expression might be relatively low or confined to a small subset of ECs, making it difficult to detect in single-cell transcriptomic datasets (49). Discrepancies between transcriptomic profiling and experimental validation have also been reported for Piezo2. Although undetected in certain scRNA-seq studies beyond the distal colon, Piezo2 expression in the small intestine and EC cells has been confirmed by RT-PCR and immunohistochemistry (50). To the best of the authors' knowledge, this is the first *in vivo* demonstration of Piezo1 expression in colonic EC cells, providing new evidence that both Piezo1 and Piezo2 may participate in epithelial mechanotransduction and serotonin-mediated gut regulation.

The present study observed a significant reduction in Piezo1 and Piezo2 expression in EC cells of FC mice, suggesting that impaired epithelial mechanotransduction contributes to the pathophysiology of functional constipation. *In vitro*, knockdown of either Piezo1 or Piezo2 reduced the expression of the other channel, indicating a potential regulatory association, although this effect was not seen *in vivo*, probably due to differences in cellular context or compensatory mechanisms. Despite their shared mechanosensory roles, Piezo1 and Piezo2 exhibited distinct physiological effects. Piezo2 knockdown selectively impaired gastric emptying and colonic sensitivity, consistent with its involvement in 5-HT-mediated visceral afferent signaling and intersegmental reflex regulation (41).

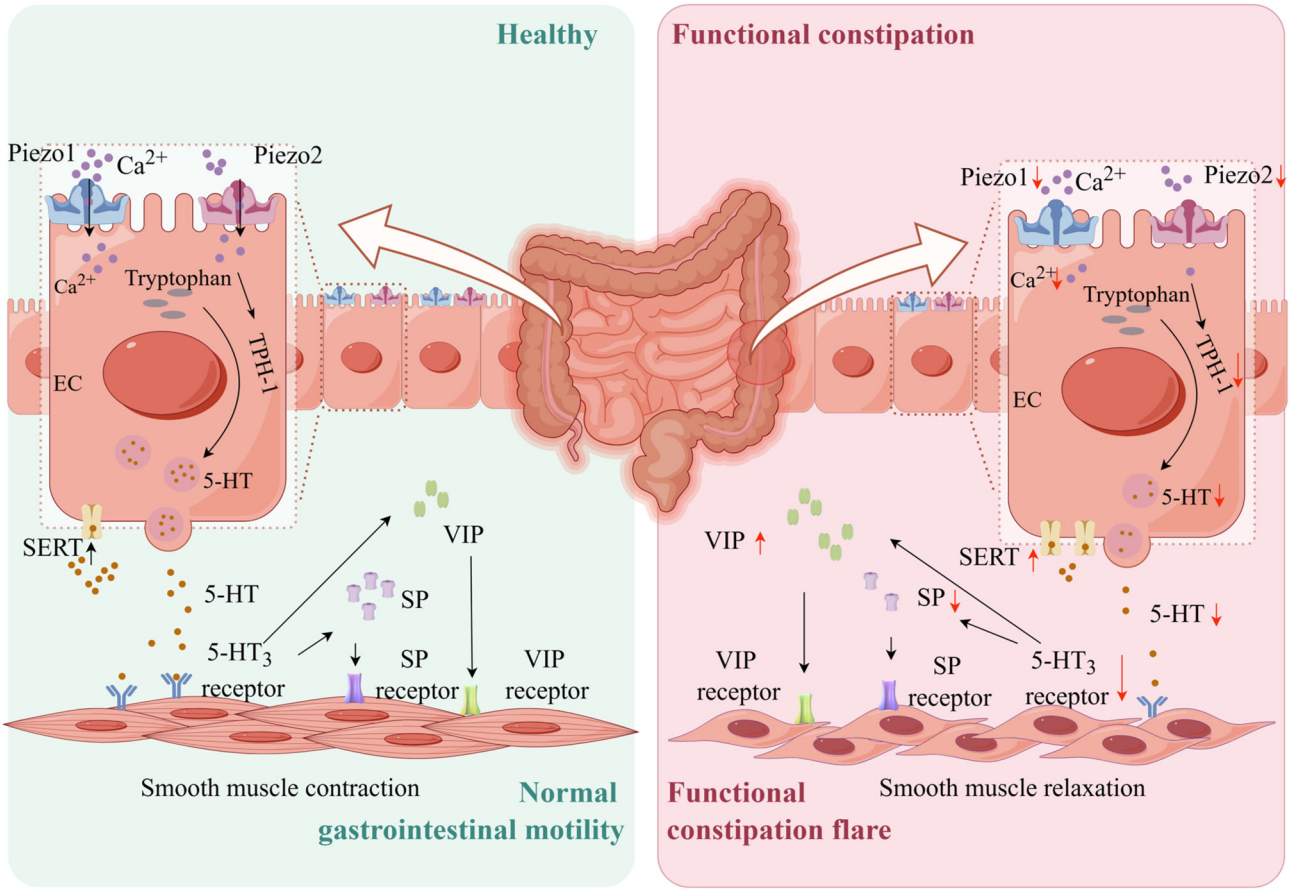

Figure 8. Mechanism diagram of the study. In functional constipation, Piezo1 and Piezo2 expression is downregulated, reducing Ca^{2+} influx and impairing 5-HT synthesis. Consequently, diminished 5-HT release reduces activation of 5-HT_3 receptors, SP levels decrease and VIP levels increase, leading to smooth muscle relaxation. Additionally, heightened SERT activity, exacerbating the deficiency in 5-HT signaling. These disruptions collectively induce pathological alterations in intestinal structure and impaired motility, leading to functional constipation symptoms. (created by figdraw.com). 5-HT, 5-hydroxytryptamine; SP, substance P; VIP, vasoactive intestinal peptide; SERT, serotonin transporter; EC, enterochromaffin cell.

By contrast, Piezo1 knockdown mainly reduced fecal water content, possibly reflecting its role in epithelial ion transport and contractile regulation (51-53). These results suggested a functional divergence: Piezo2 is more associated with sensory signaling, while Piezo1 contributes to fluid homeostasis and motility. Dual knockdown led to exacerbated gastrointestinal dysfunction, with delayed total transit, reduced fecal hydration and structural abnormalities. Although knockdown was confined to the colon, changes in gastric and small intestinal transit were observed, probably mediated by gut-brain-gut reflexes initiated by altered colonic 5-HT signaling. While colonic transit time was not directly assessed, the significant delay in total gastrointestinal transit, accompanied by reduced fecal output and water content, strongly suggested impaired colonic transport. Previous studies have directly demonstrated the critical role of Piezo channels in colonic propulsion: Piezo2 deletion in sensory neurons significantly delays colonic transit (41) and enteric Piezo1 ablation impairs colonic propulsion via disruption of neuroimmune homeostasis (44).

In the present study, serum SP levels were significantly decreased only following simultaneous knockdown of Piezo1 and Piezo2, whereas VIP levels increased with Piezo2 knockdown and were further elevated in the dual knockdown group. These results suggested that disruption of both Piezo channels may be required to perturb specific neuropeptide regulatory pathways. A similar cooperative interaction between Piezo1 and Piezo2 has been reported in other mechanotransduction contexts, such as bladder urothelium (54), supporting the plausibility of such cooperative regulation in the gut. Given the established roles of SP in promoting smooth muscle contraction and visceral sensitivity and VIP in facilitating smooth muscle relaxation and intestinal secretion (55-57), these neuropeptide changes are consistent with impaired motility and dysregulated autonomic signaling in FC.

EC cells, the main source of 5-HT in the gut, serve as mechanosensors that convert physical stimuli into chemical signals (58). Previous studies have established Piezo2 as a key transducer of mechanical forces in EC cells, promoting calcium influx and stimulating 5-HT synthesis and release via TPH-1 activation (21,59). By contrast, the role of Piezo1 in EC cells has remained unclear. Prior evidence largely limited to epithelial responses under inflammatory or immune conditions (28), with no direct data confirming its expression or function in EC cells. The present study filled this gap by providing the first direct *in vivo* and *in vitro* evidence that both Piezo1 and Piezo2 are expressed in colonic EC cells and act in a coordinated manner to regulate 5-HT signaling. Notably, genetic knockdown of either channel impaired calcium responses and reduced 5-HT synthesis and secretion, but dual knockdown led to more pronounced suppression of calcium

levels, TPH-1 expression and 5-HT production, suggesting a cooperative interaction between Piezo1 and Piezo2 in regulating EC cell mechanotransduction. While previous pharmacological studies using GsMTx4 supported a role for mechanosensitive channels in 5-HT release, they lacked specificity between Piezo isoforms (59). To overcome this limitation, our subtype-specific knockdown under both physiological and pathological conditions enabled a more precise dissection of the roles of Piezo1 and Piezo2 in regulating serotonergic signaling. Specifically, Piezo knockdown led to a reduction in 5-HT synthesis and downregulation of SERT expression, indicating disrupted serotonergic signaling. Given that serotonin exerts its effects through multiple receptor subtypes (such as 5-HT_3 and 5-HT_4) to coordinate intestinal motility and visceral sensitivity, these disruptions may contribute to the observed dysmotility and hyposensitivity in functional constipation. Moreover, the present study examined the phosphorylation status of ERK1/2 and PKC. ERK1/2 and PKC are both well-established calcium-sensitive kinases that have been reported in previous studies to be activated by Piezo1-mediated Ca^{2+} influx under mechanical or chemical stimulation (23,60). The present study showed that Piezo1 or Piezo2 knockdown significantly reduced ERK1/2 and PKC phosphorylation in colonic tissues, suggesting that Piezo channels may regulate serotonergic output via calcium-dependent kinase pathways. Nonetheless, without CaMKII data, the downstream signaling cascade remains incompletely characterized and additional studies are needed to dissect the specific contributions of distinct calcium-dependent kinases.

Current therapies for functional constipation, such as the 5-HT_4 receptor agonist prucalopride, offer symptomatic relief by enhancing colonic motility through enteric neuronal activation (61). However, their clinical efficacy remains modest, with a substantial proportion of patients exhibiting limited response (62). In addition, prucalopride is associated with systemic adverse effects (63), including headache, abdominal pain, nausea and diarrhea, which may lead to treatment discontinuation in some cases. More importantly, these agents act downstream of the serotonergic pathway and do not target upstream mechanisms such as impaired serotonin synthesis or release from enterochromaffin cells, which may underlie persistent symptoms in certain patients. By contrast, Piezo channels, serve as mechanosensitive regulators that directly influence both 5-HT production and secretion. Their rapid activation kinetics, cell-type-specific expression and dual roles in modulating gastrointestinal motility and visceral sensation support their potential as more physiologically relevant and precisely targeted therapeutic candidates (64). These features make Piezo-targeted strategies a promising complement or alternative to existing serotonergic therapies, particularly in patients who fail to respond adequately to current treatment.

Although the present study revealed the complementary roles of Piezo1 and Piezo2 in regulating the dynamics of 5-HT release and in maintaining GI homeostasis, it has some limitations. First, only the loperamide-induced constipation model was used. While this model reliably reproduces core features of functional constipation, including delayed transit and serotonergic dysregulation, it does not fully capture the multifactorial nature of the disease. Complementary models, such as those induced by low-fiber diet or aging, may enhance translational relevance in future studies. Second, the QGP-1 cell line, though widely adopted as an EC cell model (65), is derived from pancreatic endocrine tumors and may not fully reflect the characteristics of native colonic EC cells. Primary EC cells or intestinal organoids could offer greater physiological relevance. Third, while calcium imaging showed reduced intracellular calcium levels after Piezo knockdown, direct mechanical stimulation was not applied. This limits the ability to directly confirm mechanosensitive properties. Incorporating real-time mechanical stimulation would help validate Piezo channel function more conclusively. Finally, although AAV-mediated knockdown via enema allows for efficient gene delivery to the colonic epithelium, it does not offer cell-type specificity. Therefore, off-target effects on other epithelial cell types cannot be entirely ruled out. Future work employing EC cell-specific promoters or conditional knockout models will help to refine the cellular specificity of Piezo-related mechanisms.

To visually summarize the mechanistic insights derived from our findings, a schematic diagram is presented in Fig. 8. It illustrates how downregulation of Piezo1 and Piezo2 in EC cells reduces Ca^{2+} influx and 5-HT synthesis, disrupts serotonergic and neuropeptide signaling (increased VIP, decreased SP and enhanced SERT) and ultimately leads to impaired intestinal motility characteristic of functional constipation.

In conclusion, the present study revealed that Piezo1 and Piezo2 play critical and cooperative roles in maintaining GI homeostasis and regulating 5-HT signaling in the context of FC. *In vivo*, knockdown of Piezo1 or Piezo2 reduced 5-HT synthesis and release, leading to impaired intestinal motility, while *in vitro* experiments demonstrated that both channels contribute to calcium influx and 5-HT secretion. Moreover, Piezo knockdown suppressed ERK and PKC phosphorylation, indicating their involvement in calcium-activated downstream signaling pathways. These results suggested that Piezo1 and Piezo2 may represent promising therapeutic targets in intestinal motility disorders such as FC. Future research should investigate the underlying molecular mechanisms of the interactions between Piezo1 and Piezo2 and evaluate their therapeutic potential in clinical settings.

Acknowledgements

Not applicable.

Funding

The present study was supported by the National Natural Science Foundation of China (grant no. 82274652).

Availability of data and materials

The data generated in the present study may be requested from the corresponding author.

Authors' contributions

YL was responsible for conceptualization, funding acquisition, writing, reviewing and editing. JYe was responsible for methodology and project administration. XY and PM

were responsible for writing the original draft, investigation, formal analysis and data curation. WW, WZ, YL and YH were responsible for investigation and formal analysis. JYao, QZ and WZ were responsible for visualization and validation. XY and JYao confirm the authenticity of all the raw data. All authors read and approved the final manuscript.

Ethics approval and consent to participate

All animal experiments were conducted in accordance with ethical guidelines and were approved by the Animal Experiment Ethics Committee of Chengdu University of Traditional Chinese Medicine (approval no. 2024012).

Patient consent for publication

Not applicable.

Competing interests

The authors declare that they have no competing interests.

References

1. Black CJ, Drossman DA, Talley NJ, Ruddy J and Ford AC: Functional gastrointestinal disorders: Advances in understanding and management. Lancet 396: 1664-1674, 2020.
2. Ma C, Congly SE, Novak KL, Belletrutti PJ, Raman M, Woo M, Andrews CN and Nasser Y: Epidemiologic burden and treatment of chronic symptomatic functional bowel disorders in the United States: A nationwide analysis. Gastroenterology 160: 88-98.e4, 2021.
3. Rao SSC, Rattanakovit K and Patcharatrakul T: Diagnosis and management of chronic constipation in adults. Nat Rev Gastroenterol Hepatol 13: 295-305, 2016.
4. Barberio B, Judge C, Savarino EV and Ford AC: Global prevalence of functional constipation according to the Rome criteria: A systematic review and meta-analysis. Lancet Gastroenterol Hepatol 6: 638-648, 2021.
5. Palsson OS, Whitehead W, Törnblom H, Sperber AD and Simren M: Prevalence of Rome IV functional bowel disorders among adults in the United States, Canada, and the United Kingdom. Gastroenterology 158: 1262-1273.e3, 2020.
6. Rossen ND, Touhara KK, Castro J, Harrington AM, Caraballo SG, Deng F, Li Y, Brierley SM and Julius D: Population imaging of enterochromaffin cell activity reveals regulation by somatostatin. Proc Natl Acad Sci USA 122: e2501525122, 2025.
7. Bellono NW, Bayrer JR, Leitch DB, Castro J, Zhang C, O'Donnell TA, Brierley SM, Ingraham HA and Julius D: Enterochromaffin cells are gut chemosensors that couple to sensory neural pathways. Cell 170: 185-198.e16, 2017.
8. Chen Z, Luo J, Li J, Kim G, Stewart A, Urban JF Jr, Huang Y, Chen S, Wu LG, Chesler A, *et al*: Interleukin-33 promotes serotonin release from enterochromaffin cells for intestinal homeostasis. Immunity 54: 151-163.e6, 2021.
9. Kieslich B, Weiße RH, Brendler J, Ricken A, Schöneberg T and Sträter N: The dimerized pentraxin-like domain of the adhesion G protein-coupled receptor 112 (ADGRG4) suggests function in sensing mechanical forces. J Biol Chem 299: 105356, 2023.
10. Bayrer JR, Castro J, Venkataraman A, Touhara KK, Rossen ND, Morrie RD, Maddern J, Hendry A, Braverman KN, Garcia-Caraballo S, *et al*: Gut enterochromaffin cells drive visceral pain and anxiety. Nature 616: 137-142, 2023.
11. Strege PR, Knutson K, Eggers SJ, Li JH, Wang F, Linden D, Szurszewski JH, Milescu L, Leiter AB, Farrugia G and Beyder A: Sodium channel $Na_v1.3$ is important for enterochromaffin cell excitability and serotonin release. Sci Rep 7: 15650, 2017.
12. Leiser SF, Miller H, Rossner R, Fletcher M, Leonard A, Primitivo M, Rintala N, Ramos FJ, Miller DL and Kaeberlein M: Cell nonautonomous activation of flavin-containing monooxygenase promotes longevity and health span. Science 350: 1375-1378, 2015.
13. Raouf Z, Steinway SN, Scheese D, Lopez CM, Duess JW, Tsuboi K, Sampah M, Klerk D, El Baassiri M, Moore H, *et al*: Colitis-induced small intestinal hypomotility is dependent on enteroendocrine cell loss in mice. Cell Mol Gastroenterol Hepatol 18: 53-70, 2024.
14. Bhattarai Y, Williams BB, Battaglioli EJ, Whitaker WR, Till L, Grover M, Linden DR, Akiba Y, Kandimalla KK, Zachos NC, *et al*: Gut microbiota-produced tryptamine activates an epithelial G-protein-coupled receptor to increase colonic secretion. Cell Host Microbe 23: 775-785.e5, 2018.
15. Zhao J, Zhao L, Zhang S and Zhu C: Modified Liu-Jun-Zi decoction alleviates visceral hypersensitivity in functional dyspepsia by regulating EC cell-5HT3r signaling in duodenum. J Ethnopharmacol 250: 112468, 2020.
16. Nygaard A, Zachariassen LG, Larsen KS, Kristensen AS and Loland CJ: Fluorescent non-canonical amino acid provides insight into the human serotonin transporter. Nat Commun 15: 9267, 2024.
17. Wei L, Singh R, Ha SE, Martin AM, Jones LA, Jin B, Jorgensen BG, Zogg H, Chervo T, Gottfried-Blackmore A, *et al*: Serotonin deficiency is associated with delayed gastric emptying. Gastroenterology 160: 2451-2466.e19, 2021.
18. Cremon C, Carini G, Wang B, Vasina V, Cogliandro RF, De Giorgio R, Stanghellini V, Grundy D, Tonini M, De Ponti F, *et al*: Intestinal serotonin release, sensory neuron activation, and abdominal pain in irritable bowel syndrome. Am J Gastroenterol 106: 1290-1298, 2011.
19. Jin B, Ha SE, Wei L, Singh R, Zogg H, Clemmensen B, Heredia DJ, Gould TW, Sanders KM and Ro S: Colonic motility is improved by the activation of $5\text{-}HT_{2B}$ receptors on interstitial cells of cajal in diabetic mice. Gastroenterology 161: 608-622.e7, 2021.
20. Nan N, Gong MX, Wang Q, Li MJ, Xu R, Ma Z, Wang SH, Zhao H and Xu YS: Wuzhuyu decoction relieves hyperalgesia by regulating central and peripheral 5-HT in chronic migraine model rats. Phytomedicine 96: 153905, 2022.
21. Alcaino C, Knutson KR, Treichel AJ, Yildiz G, Strege PR, Linden DR, Li JH, Leiter AB, Szurszewski JH, Farrugia G and Beyder A: A population of gut epithelial enterochromaffin cells is mechanosensitive and requires Piezo2 to convert force into serotonin release. Proc Natl Acad Sci USA 115: E7632-E7641, 2018.
22. Kefauver JM, Ward AB and Patapoutian A: Discoveries in structure and physiology of mechanically activated ion channels. Nature 587: 567-576, 2020.
23. Gudipaty SA, Lindblom J, Loftus PD, Redd MJ, Edes K, Davey CF, Krishnegowda V and Rosenblatt J: Mechanical stretch triggers rapid epithelial cell division through Piezo1. Nature 543: 118-121, 2017.
24. Baghdadi MB, Houtekamer RM, Perrin L, Rao-Bhatia A, Whelen M, Decker L, Bergert M, Pérez-Gonzàlez C, Bouras R, Gropplero G, *et al*: PIEZO-dependent mechanosensing is essential for intestinal stem cell fate decision and maintenance. Science 386: eadj7615, 2024.
25. Ma S, Dubin AE, Zhang Y, Mousavi SAR, Wang Y, Coombs AM, Loud M, Andolfo I and Patapoutian A: A role of PIEZO1 in iron metabolism in mice and humans. Cell 184: 969-982.e13, 2021.
26. Swain SM and Liddle RA: Mechanosensing Piezo channels in gastrointestinal disorders. J Clin Invest 133: e171955, 2023.
27. He H, Zhou J, Xu X, Zhou P, Zhong H and Liu M: Piezo channels in the intestinal tract. Front Physiol 15: 1356317, 2024.
28. Sugisawa E, Takayama Y, Takemura N, Kondo T, Hatakeyama S, Kumagai Y, Sunagawa M, Tominaga M and Maruyama K: RNA sensing by gut Piezo1 is essential for systemic serotonin synthesis. Cell 182: 609-624.e21, 2020.
29. Ma T, Li Y, Yang N, Wang H, Shi X, Liu Y, Jin H, Kwok LY, Sun Z and Zhang H: Efficacy of a postbiotic and its components in promoting colonic transit and alleviating chronic constipation in humans and mice. Cell Rep Med 6: 102093, 2025.
30. Xu MM, Guo Y, Chen Y, Zhang W, Wang L and Li Y: Electro-acupuncture promotes gut motility and alleviates functional constipation by regulating gut microbiota and increasing butyric acid generation in mice. J Integr Med 21: 397-406, 2023.
31. Lewis SJ and Heaton KW: Stool form scale as a useful guide to intestinal transit time. Scand J Gastroenterol 32: 920-924, 1997.
32. Segura MM, Mangion M, Gaillet B and Garnier A: New developments in lentiviral vector design, production and purification. Expert Opin Biol Ther 13: 987-1011, 2013.
33. Livak KJ and Schmittgen TD: Analysis of relative gene expression data using real-time quantitative PCR and the 2(-Delta Delta C(T)) method. Methods 25: 402-408, 2001.

34. Li J, Zheng H, Liu J, Ding J, Guo Q and Zhang N: Effects of functional red pine seed direct-drinking oil on constipation and intestinal barrier function in mice. Antioxidants (Basel) 14: 14, 2024.
35. Yin J, Liang Y, Wang D, Yan Z, Yin H, Wu D and Su Q: Naringenin induces laxative effects by upregulating the expression levels of c-Kit and SCF, as well as those of aquaporin 3 in mice with loperamide-induced constipation. Int J Mol Med 41: 649-658, 2018.
36. Wu J, Lewis AH and Grandl J: Touch, tension, and transduction-the function and regulation of Piezo ion channels. Trends Biochem Sci 42: 57-71, 2017.
37. Yang X, Lin C, Chen X, Li S, Li X and Xiao B: Structure deformation and curvature sensing of PIEZO1 in lipid membranes. Nature 604: 377-383, 2022.
38. Passini FS, Jaeger PK, Saab AS, Hanlon S, Chittim NA, Arlt MJ, Ferrari KD, Haenni D, Caprara S, Bollhalder M, *et al*: Shear-stress sensing by PIEZO1 regulates tendon stiffness in rodents and influences jumping performance in humans. Nat Biomed Eng 5: 1457-1471, 2021.
39. Huang Y, Mo H, Yang J, Gao L, Tao T, Shu Q, Guo W, Zhao Y, Lyu J, Wang Q, *et al*: Mechano-regulation of GLP-1 production by Piezo1 in intestinal L cells. Elife 13: RP97854, 2024.
40. Liu Y, Fang F, Xiong Y, Wu J, Li X, Li G, Bai T, Hou X and Song J: Reprogrammed fecal and mucosa-associated intestinal microbiota and weakened mucus layer in intestinal goblet cell-specific Piezo1-deficient mice. Front Cell Infect Microbiol 12: 1035386, 2022.
41. Servin-Vences MR, Lam RM, Koolen A, Wang Y, Saade DN, Loud M, Kacmaz H, Frausto S, Zhang Y, Beyder A, *et al*: PIEZO2 in somatosensory neurons controls gastrointestinal transit. Cell 186: 3386-3399, 2023.
42. Xu Y, Xiong Y, Liu Y, Li G, Bai T, Zheng G, Hou X and Song J: Activation of goblet cell Piezo1 alleviates mucus barrier damage in mice exposed to WAS by inhibiting H3K9me3 modification. Cell Biosci 13: 7, 2023.
43. Chang JE, Buechler MB, Gressier E, Turley SJ and Carroll MC: Mechanosensing by Peyer's patch stroma regulates lymphocyte migration and mucosal antibody responses. Nat Immunol 20: 1506-1516, 2019.
44. Xie Z, Rose L, Feng J, Zhao Y, Lu Y, Kane H, Hibberd TJ, Hu X, Wang Z, Zang K, *et al*: Enteric neuronal Piezo1 maintains mechanical and immunological homeostasis by sensing force. Cell 188: 2417-2432.e19, 2025.
45. Swain SM, Romac JMJ, Shahid RA, Pandol SJ, Liedtke W, Vigna SR and Liddle RA: TRPV4 channel opening mediates pressure-induced pancreatitis initiated by Piezo1 activation. J Clin Invest 130: 2527-2541, 2020.
46. Borbiro I, Badheka D and Rohacs T: Activation of TRPV1 channels inhibits mechanosensitive Piezo channel activity by depleting membrane phosphoinositides. Sci Signal 8: ra15, 2015.
47. Xie Z, Feng J, Hibberd TJ, Chen BN, Zhao Y, Zang K, Hu X, Yang X, Chen L, Brookes SJ, *et al*: Piezo2 channels expressed by colon-innervating TRPV1-lineage neurons mediate visceral mechanical hypersensitivity. Neuron 111: 526-538.e4, 2023.
48. Song Y, Fothergill LJ, Lee KS, Liu BY, Koo A, Perelis M, Diwakarla S, Callaghan B, Huang J, Wykosky J, *et al*: Stratification of enterochromaffin cells by single-cell expression analysis. Elife 12: RP90596, 2025.
49. Kharchenko PV, Silberstein L and Scadden DT: Bayesian approach to single-cell differential expression analysis. Nat Methods 11: 740-742, 2014.
50. Wang F, Knutson K, Alcaino C, Linden DR, Gibbons SJ, Kashyap P, Grover M, Oeckler R, Gottlieb PA, Li HJ, *et al*: Mechanosensitive ion channel Piezo2 is important for enterochromaffin cell response to mechanical forces. J Physiol 595: 79-91, 2017.
51. Qian W, Hadi T, Silvestro M, Ma X, Rivera CF, Bajpai A, Li R, Zhang Z, Qu H, Tellaoui RS, *et al*: Microskeletal stiffness promotes aortic aneurysm by sustaining pathological vascular smooth muscle cell mechanosensation via Piezo1. Nat Commun 13: 512, 2022.
52. Bi Y, Li H, Diao M, Liu Q, Huang L, Tao Y, Wan Y and Lin X: Piezo1 overexpression in the uterus contributes to myometrium contraction and inflammation-associated preterm birth. J Transl Med 22: 1140, 2024.
53. Luo M, Gu R, Wang C, Guo J, Zhang X, Ni K, Liu L, Pan Y, Li J and Deng L: High stretch associated with mechanical ventilation promotes piezo1-mediated migration of airway smooth muscle cells. Int J Mol Sci 25: 1748, 2024.
54. Dalghi MG, Ruiz WG, Clayton DR, Montalbetti N, Daugherty SL, Beckel JM, Carattino MD and Apodaca G: Functional roles for PIEZO1 and PIEZO2 in urothelial mechanotransduction and lower urinary tract interoception. JCI Insight 6: e152984, 2021.
55. Bai X, De Palma G, Boschetti E, Nishiharo Y, Lu J, Shimbori C, Costanzini A, Saqib Z, Kraimi N, Sidani S, *et al*: Vasoactive intestinal polypeptide plays a key role in the microbial-neuro-immune control of intestinal motility. Cell Mol Gastroenterol Hepatol 17: 383-398, 2024.
56. Talbot J, Hahn P, Kroehling L, Nguyen H, Li D and Littman DR: Feeding-dependent VIP neuron-ILC3 circuit regulates the intestinal barrier. Nature 579: 575-580, 2020.
57. Yin Y, Zhong L, Wang JW, Zhao XY, Zhao WJ and Kuang HX: Tong Xie Yao Fang relieves irritable bowel syndrome in rats via mechanisms involving regulation of 5-hydroxytryptamine and substance P. World J Gastroenterol 21: 4536-4546, 2015.
58. Chin A, Svejda B, Gustafsson BI, Granlund AB, Sandvik AK, Timberlake A, Sumpio B, Pfragner R, Modlin IM and Kidd M: The role of mechanical forces and adenosine in the regulation of intestinal enterochromaffin cell serotonin secretion. Am J Physiol Gastrointest Liver Physiol 302: G397-G405, 2012.
59. Zhu Z, Chen X, Chen S, Hu C, Guo R, Wu Y, Liu Z, Shu X and Jiang M: Examination of the mechanism of Piezo ion channel in 5-HT synthesis in the enterochromaffin cell and its association with gut motility. Front Endocrinol (Lausanne) 14: 1193556, 2023.
60. Caulier A, Jankovsky N, Demont Y, Ouled-Haddou H, Demagny J, Guitton C, Merlusca L, Lebon D, Vong P, Aubry A, *et al*: PIEZO1 activation delays erythroid differentiation of normal and hereditary xerocytosis-derived human progenitor cells. Haematologica 105: 610-622, 2020.
61. Garnock-Jones KP: Prucalopride: A review in chronic idiopathic constipation. Drugs 76: 99-110, 2016.
62. Mugie SM, Korczowski B, Bodi P, Green A, Kerstens R, Ausma J, Ruth M, Levine A and Benninga MA: Prucalopride is no more effective than placebo for children with functional constipation. Gastroenterology 147: 1285-1295.e1, 2014.
63. Chang L, Chey WD, Imdad A, Almario CV, Bharucha AE, Diem S, Greer KB, Hanson B, Harris LA, Ko C, *et al*: American gastroenterological association-american college of gastroenterology clinical practice guideline: Pharmacological management of chronic idiopathic constipation. Gastroenterology 164: 1086-1106, 2023.
64. Liu S, Yang X, Chen X, Zhang X, Jiang J, Yuan J, Liu W, Wang L, Zhou H, Wu K, *et al*: An intermediate open structure reveals the gating transition of the mechanically activated PIEZO1 channel. Neuron 113: 590-604.e6, 2025.
65. Doihara H, Nozawa K, Kojima R, Kawabata-Shoda E, Yokoyama T and Ito H: QGP-1 cells release 5-HT via TRPA1 activation; a model of human enterochromaffin cells. Mol Cell Biochem 331: 239-245, 2009.